Tumor growth at the primary site and body weight were continuously monitored. Intratumoral injection of OBP-301 in both regimens induced a gradual reduction in tumor volumes compared with mock-treated mice. Mice with tumor shrinkage significantly recovered body weight starting on day 10 (regimen 1) or day 15 (regimen 2) after the last virus injection ($P < 0.05$), although there was a decrease in body weight in the control group (Fig. 3D). This antitumor effect could be observed in mice orthotopically implanted with HSC-3 cells; the appearance of the effect, however, was ~4 to 5 days slower than that of SAS-L tumor-bearing mice (Supplementary Fig. S4).

Locoregional spread of virus following virotherapy in an orthotopic human SCCHN model. SCCHN patients with metastases to regional lymph nodes have a poorer prognosis than patients without nodal metastases (16). To verify whether adenoviruses could traffic to regional lymph nodes through the lymphatics, we injected 1×10^8 pfu of OBP-401 into SAS-L tumors implanted into the tongues of mice. Five days after virus injection, primary tongue tumors as well as lymph node metastases could be detected as light-emitting spots with GFP fluorescence under the optical charge-coupled device imaging (Fig. 5A). We also found that OBP-401 could infect and replicate in SAS-L cells trafficking in lymphatic vessels (Fig. 5B). These results suggest that although adenoviruses could effectively drain to regional lymph nodes, OBP-401 replicated only in metastatic lymph nodes, which was confirmed by a histopathologic analysis. Metastatic SCCHN cells were mostly observed in the lymph nodes with fluorescence emission, whereas most of GFP-negative lymph nodes contained no tumor cells (Fig. 5C). The optical imaging detected 13 lymph nodes labeled in spots with GFP fluorescence in 14 metastatic nodes (sensitivity of 92.9%). Among 21 metastasis-free lymph nodes, 3 nodes were GFP positive (specificity of 85.7%). In another orthotopic model implanted with HSC-3 human SCCHN cells, we could also detect GFP signals in one or two metastatic lymph nodes but not in other nonmetastatic nodes and salivary glands (Fig. 5; Supplementary Fig. S5).

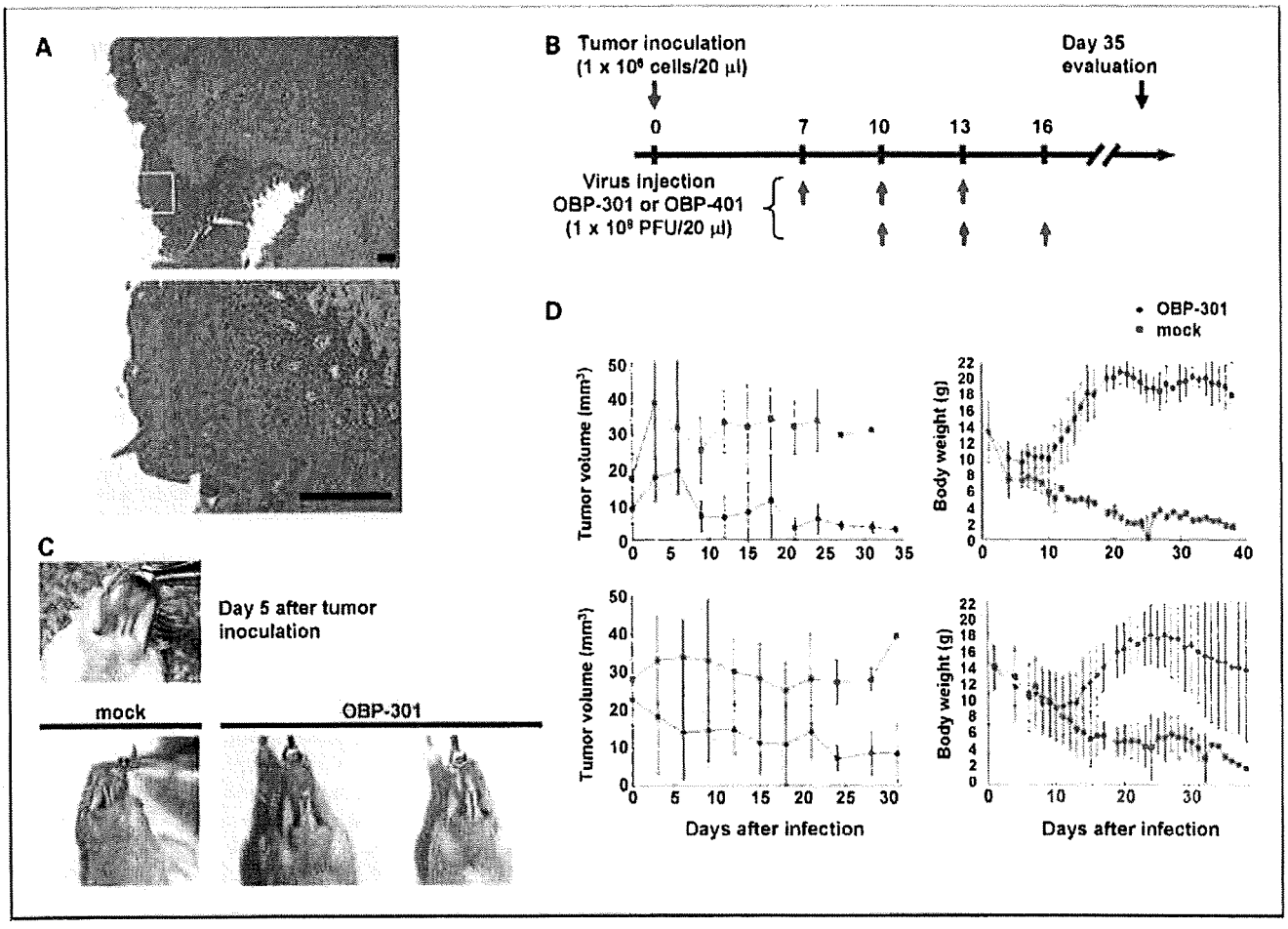

Fig. 3. Antitumor effects of OBP-301 *in vivo* in an orthotopic SCCHN model. *A*, tumor sections were obtained 35 d after tumor cell implantation. Paraffin-embedded sections of SAS-L tongue tumors were stained with H&E. Scale bar, 100 μm. Top, ×40 magnification; bottom, detail of the boxed region of the top panel; magnification, ×400. *B*, orthotopic animal experiment regimens. The tongues of BALB/c *nu/nu* mice were inoculated with 1×10^5 SAS-L human SCCHN cells. Orthotopic tumor-bearing mice received three courses of intratumoral injection of 1×10^8 pfu of viruses every 3 d starting on day 7 (regimen 1) or day 10 (regimen 2) after tumor cell inoculation. Eight mice were used in each group. *C*, macroscopic appearance of SAS-L tongue tumors on BALB/c *nu/nu* mice 5 d (*top*) or 35 d (*bottom*) after tumor cell inoculation. Representative tumors treated with PBS or OBP-301 are shown. Note the eradicated tumors in mice that received OBP-301 injection. Green arrowhead, SAS-L tumors. *D*, orthotopic tumor-bearing mice received three courses of intratumoral injection of 1×10^8 pfu of viruses every 3 d starting on day 7 (regimen 1; *top*) or day 10 (regimen 2; *bottom*) after tumor cell inoculation. The tumor volume (*left*) and the body weight (*right*) were monitored and plotted. Point, mean; bars, SD. Statistical significance was defined as $P < 0.05$.

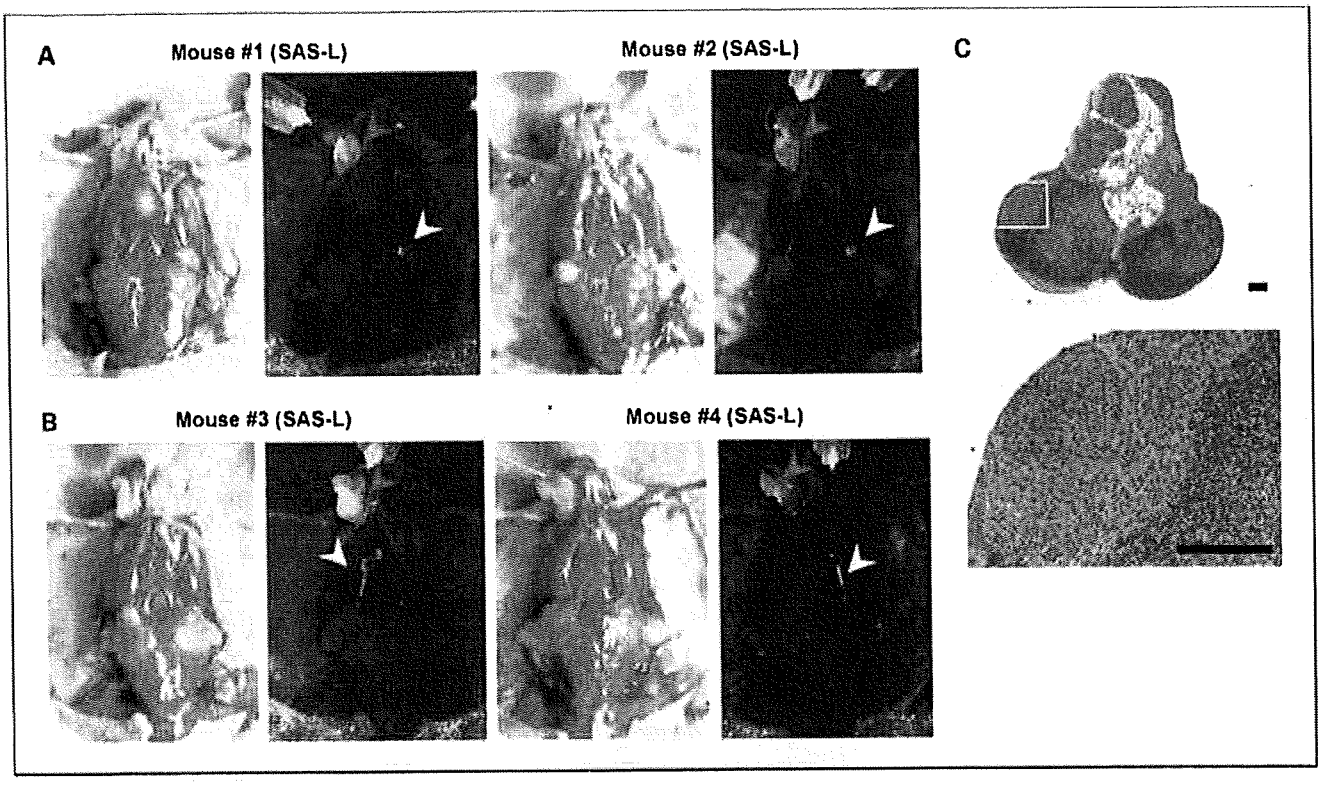

Fig. 4. Virus spread of OBP-401 via lymphatics to regional lymph nodes on SAS-L tumor-bearing mice. *A*, selective visualization of lymph node metastasis in orthotopic xenografts of SAS-L human SCCHN cells. Mice received intratumoral injection of OBP-401 (1×10^8 pfu) 24 d after tumor inoculation and were assessed for lymph node metastasis 5 d later under charge-coupled device imaging. Left, gross appearance; right, fluorescence image. Red arrowhead, primary tumor; white arrowhead, metastatic tumor cells. *B*, selective visualization of lymph node metastasis and lymphatic dissemination in orthotopic xenografts of SAS-L cells. Note the GFP-expressing disseminated tumor cells in lymphatics. Red arrowhead, primary tumor; white arrowhead, metastatic tumor cells in lymphatics. *C*, sections of GFP-positive lymph nodes were obtained 35 d after tumor cell implantation. Paraffin-embedded sections of lymph nodes were stained with H&E. Scale bar, 100 μm.

Prolonged survival following OBP-301 virotherapy in an orthotopic human SCCHN model. Finally, we assessed the effect of intratumoral injection of OBP-301 on survival time of SAS-L–bearing mice. Mice treated with OBP-301 beginning either on the 7th day (regimen 1) or the 10th day (regimen 2) after tumor implantation survived significantly longer (mean = 27.4 or 33.7 days) than mice without treatment (mean = 14.7 or 24.3 days; regimen 1, $P = 0.017$; regimen 2, $P = 0.016$; Fig. 6). The prolonged survival might reflect an antitumor effect of oncolytic adenoviruses spreading into the locoregional area, including regional lymph nodes.

Discussion

The present study illustrates the potential application of replication-selective oncolytic adenoviruses as an anticancer agent in human SCCHN patients. We found that intratumoral administration of telomerase-specific oncolytic adenovirus induced tumor volume reduction as well as the recovery of weight loss by enabling oral ingestion in an orthotopic xenograft model, in which human SCCHN cells were implanted into the tongues of BALB/c *nu/nu* mice. Oncolytic virotherapy also prolonged the survival of SCCHN tumor-bearing mice, presumably due to the locoregional antitumor effect against primary tumors and lymph node metastases with viruses spreading into the lymphatics.

Telomerase-specific oncolytic adenovirus OBP-301 exhibits a broad cytopathic effect against human cancer cell lines of different tissue origins (8–10). In a panel of human SCCHN cell lines, OBP-301 also showed apparent antitumor effects *in vitro* in a dose-dependent manner (Fig. 1B), although the sensitivity varied greatly between cell lines despite hTERT and coxsackievirus and adenovirus receptor expression (Supplementary Fig. S1). We have previously found that the process of oncolysis is morphologically distinct from apoptosis and necrosis (17). The cell death machinery triggered by OBP-301 infection is still under the investigation, although autophagy is partially involved in this effect (17, 18). OBP-301 has been developed based on the ability of the hTERT promoter to control replication of the virus in the tumors, leading to selective killing of tumor cells and minimal undesired effects on normal cells; the ID_{50} values of OBP-301 in various human cancer cell lines, however, were not related to the levels of *hTERT* mRNA expression (8, 10). Indeed, HSC-3 and HSC-4 human SCCHN cells expressing high levels of *hTERT* mRNA were less sensitive to OBP-301 than SCC-4 and SCC-9 cells with low levels of hTERT expression. Thus, neither hTERT expression nor coxsackievirus and adenovirus receptor expression could be useful for predicting the outcome of OBP-301 treatment.

Biomarkers have been extensively studied and often used to predict the potential therapeutic benefit of new agents, including molecular-targeted therapies (19). There is a widely recognized need for biomarkers that could improve the

clinician's ability to select suitable drugs for appropriate patients. We found that the levels of GFP expression following OBP-401 infection were highly associated with ID_{50} values of OBP-301 in individual cell lines *in vitro* (Fig. 2C). This correlation may be an expected result, because OBP-301 and OBP-401 have the same genomic backbone except for the GFP expression cassette. Although it is necessary to establish the assay procedures for GFP-based fluorescence measurement in more detail, we propose the diagnostic application of OBP-401 to predict tumor responses to OBP-301. For example, when the biopsy tissue samples of the tumor are exposed to OBP-401 for a certain amount of time *ex vivo*, the levels of GFP expression may be of value as a positive predictive marker for the outcome of OBP-301 virotherapy. Further prospective clinical studies are required to confirm the direct correlation between the GFP expression in biopsy samples following *ex vivo* OBP-401 infection and the clinical responses to OBP-301 in patients with SCCHN.

An orthotopic nude mouse model to investigate the cellular and molecular mechanisms of metastasis in human neoplasia was first described by Fidler et al. (20, 21) and Killion et al. (22). The orthotopic implantation of tumor cells restores the correct tumor-host interactions, which do not occur when tumors are implanted in ectopic subcutaneous sites (20). To further explore the *in vivo* antitumor effects of telomerase-specific virotherapy for SCCHN, we used an orthotopic nude mouse model of human tongue squamous cell carcinoma. In our preliminary experiments, we inoculated tumor cells into the tongue of BALB/c *nu/nu* mice and confirmed the formation of tumors with a diameter of 3 to 5 mm after 5 days and the development of metastases in neck lymph nodes after 35 days. We also identified the presence of disseminated tumor cells in the regional lymph nodes at least 10 days after tumor cell implantation by using GFP-expressing SAS-L human SCCHN cells (data not shown). Intratumoral injection of OBP-301 done 7 or 10 days after tumor inoculation significantly shrunk the tongue SAS-L tumor volumes, which in turn increased the body weight of mice by enabling oral ingestion (Fig. 3D). Moreover, HSC-3 cells were relatively resistant to OBP-301 *in vitro*; intratumoral injection of OBP-301 was, however, effective for recovering the body weight in mice bearing HSC-3 tongue tumors after a long-term observation (Supplementary Fig. S4). These results suggest that although the appearance of the effect may be slower, the *in vivo* antitumor activity could be

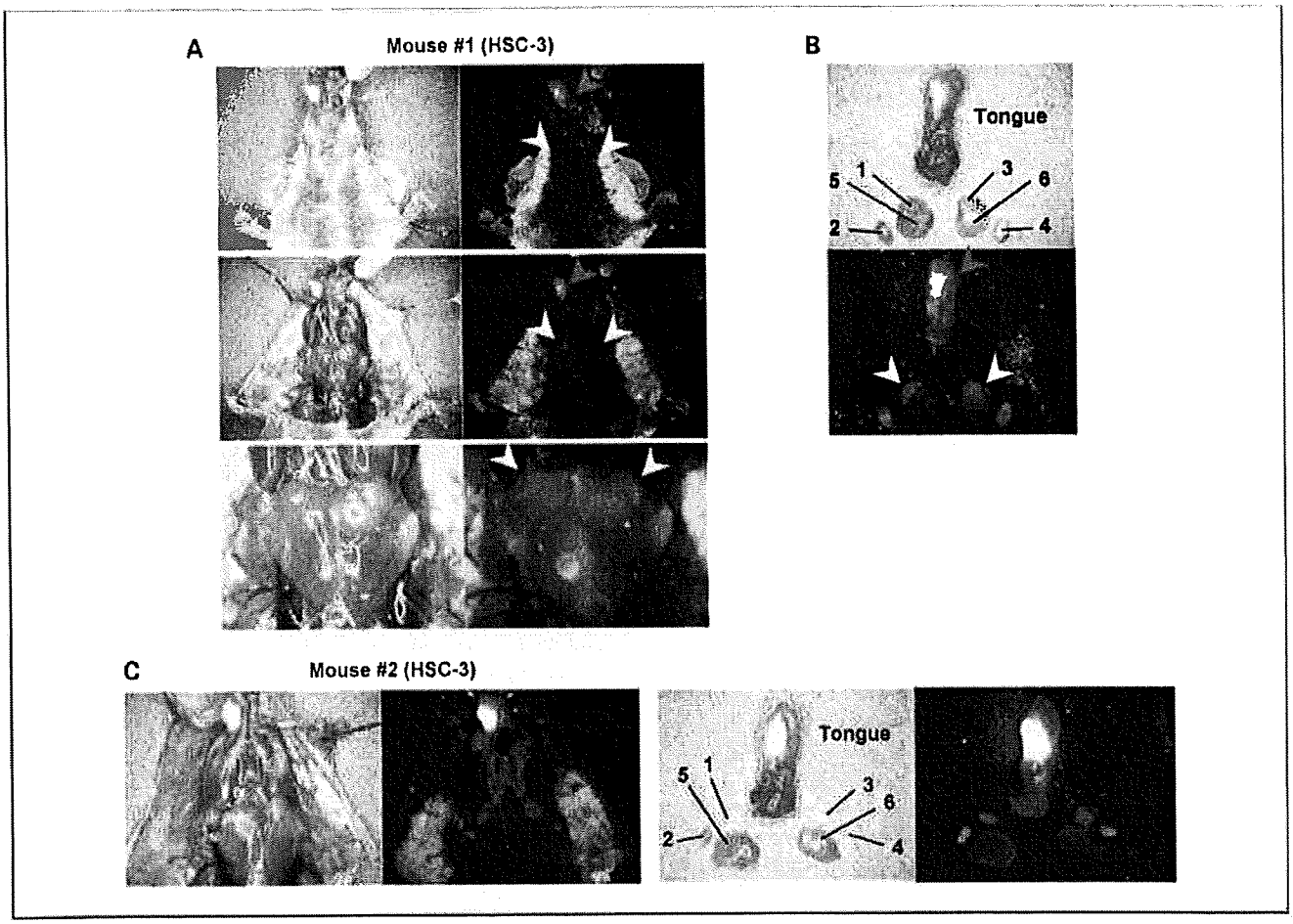

Fig. 5. Virus spread of OBP-401 via lymphatics to regional lymph nodes on HSC-3 tumor-bearing mice. *A*, selective visualization of lymph node metastasis in orthotopic xenografts of HSC-3 human SCCHN cells. Mice received intratumoral injection of OBP-401 at the concentration of 1×10^8 pfu after 24 d of tumor inoculation and were assessed for lymph node metastasis 5 d later under fluorescence stereomicroscope. *B*, HSC-3 primary tumor, salivary glands, and lymph nodes were excised 5 d after OBP-401 injection and then assessed for GFP fluorescence. 1 to 4, lymph nodes; 5 and 6, salivary glands. *C*, other HSC-3 tumor-bearing mice. Excised primary tumors, salivary glands, and lymph nodes were assessed for GFP fluorescence.

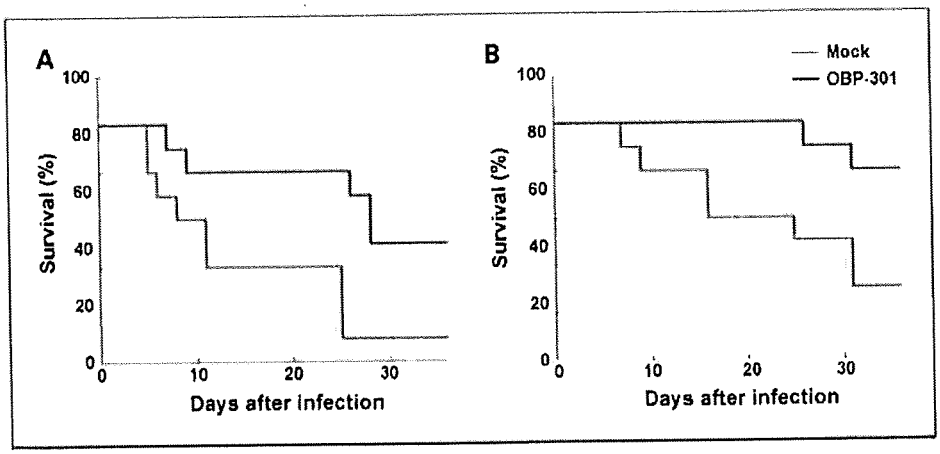

Fig. 6. Prolonged survival of SAS-L tumor-bearing mice treated with OBP-301. Mice bearing SAS-L xenografts were treated starting on day 7 (regimen 1; *A*) or day 10 (regimen 2; *B*) after tumor cell inoculation as described in Fig. 3A. Survival was monitored over time after virus injection and plotted as a Kaplan-Meier plot.

expected even in resistant SCCHN tumors. Because the body weight loss due to a feeding problem in this orthotopic SCCHN model resembles the disease progression in SCCHN patients, the finding that OBP-301 increased the body weight of mice suggests that OBP-301 virotherapy could potentially improve the quality of life in advanced SCCHN patients.

Amplified viruses can infect adjacent tumor cells as well as reach metastatic lymph nodes via the lymphatic circulation. We have previously shown that the telomerese-specific OBP-401–expressing GFP could be delivered into human tumor cells in regional lymph nodes and replicate with selective GFP fluorescence after injection into the primary tumor in an orthotopic rectal tumor model (11). In the orthotopic SCCHN model, OBP-401 spread into the neck lymph nodes after injection into the primary tongue tumor and selectively replicated in metastatic nodules (Figs. 4 and 5; Supplementary Fig. S5). The sensitivity and specificity of this imaging strategy for SAS-L tumors are 92.9% and 85.7%, respectively, which are sufficiently reliable to support the concept of this approach. These results suggest that surgeons may be able to excise primary tumors as well as metastatic lymph nodes precisely with appropriate margins by using this novel surgical navigation system with OBP-401. Moreover, the therapeutic profiles of OBP-401 and OBP-301 are considered similar, and a histopathologic analysis showed the destruction of micrometastases by virus in metastatic lymph nodes. This regional antitumor effect of oncolytic viruses could have a significant effect on the prolongation of the survival of mice bearing orthotopic tumors (Fig. 6).

Targeted therapies such as the anti–epidermal growth factor receptor monoclonal antibody cetuximab and other small-molecule epidermal growth factor receptor–tyrosine kinase inhibitors have been developed for SCCHN. Although a phase III trial showed a survival benefit with cetuximab and standard platinum-based therapy in SCCHN patients (23), some patients are exquisitely sensitive to these drugs and can develop particular and severe toxicities (24). A phase I study is currently under way in the United States to determine the feasibility and to characterize the pharmacokinetics of OBP-301 in patients with histologically proven nonresectable solid tumors (25). An interim analysis of the first 12 patients, including four SCCHN patients treated with escalating doses of OBP-301, indicates that OBP-301 virotherapy is well tolerated without any severe adverse events, suggesting that OBP-301 may be much more potent than other targeted therapies for human SCCHN in terms of specificity, efficacy, and toxicity.

In conclusion, our data clearly indicate that telomerase-specific oncolytic adenoviruses have a significant therapeutic potential against human SCCHN *in vitro* and *in vivo*. Moreover, these viruses can be used in an *ex vivo* diagnostic assay to predict the therapeutic potential of the virus in SCCHN patients. The combination of a diagnostic assay with a therapeutic entity is termed theranostics (26). Telomerase-specific oncolytic viruses can be used to treat the patients and to identify the patients who will likely benefit from virotherapy (Supplementary Fig. S6). In addition, telomerase-specific *in situ* imaging strategy has a potential of being widely available in humans as a navigation system in the surgical treatment of SCCHN. Thus, our oncolytic virus–based approach might be a novel "virotheranostics" for SCCHN. Phase II studies of telomerase-specific virotheranostics in advanced SCCHN patients are warranted.

Disclosure of Potential Conflicts of Interest

H. Onimatsu and Y. Urata are employed by Oncolys BioPharma, Inc. T. Fujiwara is a consultant to Oncolys Biopharma, Inc.

Acknowledgments

We thank Daiju Ichimaru and Hitoshi Kawamura for their helpful discussions and Tomoko Sueishi for her excellent technical support.

References

1. Parkin DM, Bray F, Ferlay J, Pisani P. Global cancer statistics, 2002. CA Cancer J Clin 2005;55:74–108.
2. Jemal A, Clegg LX, Ward E, et al. Annual report to the nation on the status of cancer, 1975–2001, with a special feature regarding survival. Cancer 2004;101:3–27.
3. Vokes EE, Weichselbaum RR, Lippman SM, Hong WK. Head and neck cancer. N Engl J Med 1993;328:184–94.
4. Vokes EE, Crawford J, Bogart J, Socinski MA, Clamon G, Green MR. Concurrent chemoradiotherapy for unresectable stage III non-small cell lung cancer. Clin Cancer Res 2005;11:5045–50s.
5. Milas L, Mason KA, Liao Z, Ang KK. Chemoradiotherapy: emerging treatment improvement strategies. Head Neck 2003;25:152–67.
6. Kirn D, Martuza RL, Zwiebel J. Replication-selective virotherapy for cancer: biological principles, risk management and future directions. Nat Med 2001;7:781–7.
7. Hawkins LK, Lemoine NR, Kirn D. Oncolytic

biotherapy: a novel therapeutic plafform. Lancet Oncol 2002;3:17–26.

8. Kawashima T, Kagawa S, Kobayashi N, et al. Telomerase-specific replication-selective virotherapy for human cancer. Clin Cancer Res 2004;10:285–92.
9. Taki M, Kagawa S, Nishizaki M, et al. Enhanced oncolysis by a tropism-modified telomerase-specific replication-selective adenoviral agent OBP-405 ('Telomelysin-RGD'). Oncogene 2005;24:3130–40.
10. Hashimoto Y, Watanabe Y, Shirakiya Y, et al. Establishment of biological and pharmacokinetic assays of telomerase-specific replication-selective adenovirus. Cancer Sci 2008;99:385–90.
11. Kishimoto H, Kojima T, Watanabe Y, et al. *In vivo* imaging of lymph node metastasis with telomerase-specific replication-selective adenovirus. Nat Med 2006;12:1213–9.
12. Kotwall C, Sako K, Razack MS, Rao U, Bakamjian V, Shedd DP. Metastatic patterns in squamous cell cancer of the head and neck. Am J Surg 1987;154: 439–42.
13. Myers JN, Holsinger FC, Jasser SA, Bekele BN, Fidler IJ. An orthotopic nude mouse model of oral tongue squamous cell carcinoma. Clin Cancer Res 2002;8:293–8.
14. Fujiwara T, Kagawa S, Kishimoto H, et al. Enhanced antitumor efficacy of telomerase-selective oncolytic adenoviral agent OBP-401 with docetaxel: preclinical evaluation of chemovirotherapy. Int J Cancer 2006; 119:432–40.
15. Riley T, Sontag E, Chen P, Levine A. Transcriptional control of human p53-regulated genes. Nat Rev Mol Cell Biol 2008;9:402–12.
16. Lefebvre JL. Current clinical outcomes demand new treatment options for SCCHN. Ann Oncol 2005;16 Suppl 6:vi7–12.
17. Endo Y, Sakai R, Ouchi M, et al. Virus-mediated oncolysis induces danger signal and stimulates cytotoxic T-lymphocyte activity via proteasome activator upregulation. Oncogene 2008;27:2375–81.
18. Ito H, Aoki H, Kühnel F, et al. Autophagic cell death of malignant glioma cells induced by a conditionally replicating adenovirus. J Natl Cancer Inst 2006;98: 625–36.
19. Sarker D, Workman P. Pharmacodynamic biomarkers for molecular cancer therapeutics. Adv Cancer Res 2007;96:213–68.
20. Fidler IJ. Rationale and methods for the use of nude mice to study the biology and therapy of human cancer metastasis. Cancer Metastasis Rev 1986;5:29–49.
21. Fidler IJ, Naito S, Pathak S. Orthotopic implantation is essential for the selection, growth and metastasis of human renal cell cancer in nude mice. Cancer Metastasis Rev 1990;9:149–65.
22. Killion JJ, Radinsky R, Fidler IJ. Orthotopic models are necessary to predict therapy of transplantable tumors in mice. Cancer Metastasis Rev 1998;17: 279–84.
23. Langer CJ. Targeted therapy in head and neck cancer: state of the art 2007 and review of clinical applications. Cancer 2008;112:2635–45.
24. Widakowich C, de Castro G, Jr., de Azambuja E, Dinh P, Awada A. Review: side effects of approved molecular targeted therapies in solid cancers. Oncologist 2007;12:1443–55.
25. Fujiwara T, Tanaka N, Nemunaitis J, et al. Phase I trial of intratumoral administration of OBP-301, a novel telomerase-specific oncolytic virus, in patients with advanced solid cancer: Evaluation of biodistribution and immune response. 2008 ASCO Annual Meeting Proceedings. J Clin Oncol 2008; 26:3572.
26. Del Vecchio S, Zannetti A, Fonti R, Pace L, Salvatore M. Nuclear imaging in cancer theranostics. Q J Nucl Med Mol Imaging 2007;51:152–63.

Telomerase-specific virotherapy in an animal model of human head and neck cancer

Oumi Nakajima,[1] Atsuko Matsunaga,[2] Daiju Ichimaru,[3] Yasuo Urata,[3] Toshiyoshi Fujiwara,[4] and Koji Kawakami[1,2]

[1]Department of Pharmacoepidemiology, Graduate School of Medicine and Public Health, Kyoto University, Kyoto, Japan; [2]Department of Advanced Clinical Science and Therapeutics, Graduate School of Medicine, University of Tokyo; [3]Oncolys Biopharma, Inc., Tokyo, Japan; and [4]Center for Gene and Cell Therapy, Okayama University Hospital, Okayama, Japan

Abstract

Telomerase-specific replication-competent adenovirus, Telomelysin (OBP-301), has a human telomerase reverse transcriptase promoter that regulates viral replication and efficiently kills human cancer cells. The objectives of this study are to examine the effects of OBP-301 in squamous cell carcinoma of the head and neck cells *in vitro* and in xenografted animals *in vivo*. OBP-301 was found to be cytotoxic to the YCUT892, KCCT873, KCCT891, KCCL871, YCUM862, HN12, and KCCOR891 cell lines *in vitro*. However, the level of cytotoxicity is not correlated with the expression levels of adenoviral receptors, which may be required for adenoviral infection in squamous cell carcinoma of the head and neck cells. OBP-301 shows remarkable antitumor activity against established s.c. KCCT873 tumors in immunodeficient animals in a dose-dependent manner. In addition, no significant toxicity was observed in animals receiving treatment. These results suggest that OBP-301 is a novel therapeutic agent with promise for the treatment of human head and neck cancers. [Mol Cancer Ther 2009;8(1):171–7]

Introduction

Squamous cell carcinoma of the head and neck (SCCHN) accounts for 5% of newly diagnosed adult cancers in the United States and 8% of cancers worldwide (1). Most patients are treated with various combinations of surgery, radiotherapy, and systemic agents (2). Despite major advances in the treatment of locoregionally advanced SCCHN, such as the introduction of novel chemotherapy regimens and inhibitors of the epidermal growth factor receptor, treatment fails in about half of the patients (3). The median survival of patients with recurrent or metastatic SCCHN who undergo chemotherapy is 6 to 9 months (4). Therefore, a considerable number of patients with SCCHN need additional treatment as the disease progresses.

Virotherapy, the approach to treat cancer with virus, has been done in some clinical trials; for example, clinical trials primarily using *p53* gene replacement (INGN-201; a replication-competent adenoviral-based vector expressing wild-type *p53*) have provided the basis for the design of ongoing randomized gene therapy clinical trials in SCCHN patients in the United States (5). Although systemic administration is probably required in the case of micrometastatic disease, virotherapy has some promise when tumor is limited to the head and neck. SCCHN is a particularly attractive model because most primary and recurrent lesions are easily acceptable to direct injection (6). Potential usage of virotherapy may include the perioperative application in the surgical wound and the addition of intratumoral (i.t.) virotherapy to current standard options, such as radiotherapy and/or chemotherapy.

Telomerase is a ribonucleoprotein complex responsible for the complete replication of chromosomal ends (7). Many studies have shown the expression of telomerase activity in >85% of human cancers (8) but only in a few normal somatic cell types (9). Telomerase activation is considered to be a critical step in carcinogenesis, and its activity is closely correlated with human telomerase reverse transcriptase (hTERT) expression (10). Therefore, the hTERT proximal promoter can be used as a molecular switch for selective expression of target genes in tumor cells. Replication-selective tumor-specific adenoviruses are being developed as novel anticancer therapies (11–14). In this context, an adenoviral vector that drives E1A and E1B genes under the hTERT promoter has been developed, termed Telomelysin or OBP-301 (15). OBP-301 can replicate in and lyse only cancer cells but not normal cells, and its strong cytotoxic activity were shown in a variety human cancer cells (15–17). Also, OBP-301-mediated oncolysis induces uric acid production as a danger signal and stimulates CTL activity via proteasome activator up-regulation (18).

The infection efficiency of recombinant adenoviral vectors varies widely depending on the expression of the primary receptor, the coxsackie adenovirus receptor (CAR); the secondary receptors, integrin $\alpha_V\beta_3$ and integrin $\alpha_V\beta_5$; and the tertiary receptor, heparan sulfate glycosaminoglycans (HSG; refs. 19, 20). The first step is the attachment of

Received 7/1/08; revised 9/26/08; accepted 10/23/08.

Grant support: Japanese Ministry of Health, Labour and Welfare grant-in-aid KH33332 (K. Kawakami).

The costs of publication of this article were defrayed in part by the payment of page charges. This article must therefore be hereby marked *advertisement* in accordance with 18 U.S.C. Section 1734 solely to indicate this fact.

Requests for reprints: Koji Kawakami, Department of Pharmacoepidemiology, Graduate School of Medicine and Public Health, Kyoto University, Yoshida Konoecho, Sakyo-ku, Kyoto 606-8501, Japan. Phone: 81-75-753-4459; Fax: 81-75-753-4469. E-mail: kawakami-k@umin.ac.jp

doi:10.1158/1535-7163.MCT-08-0620

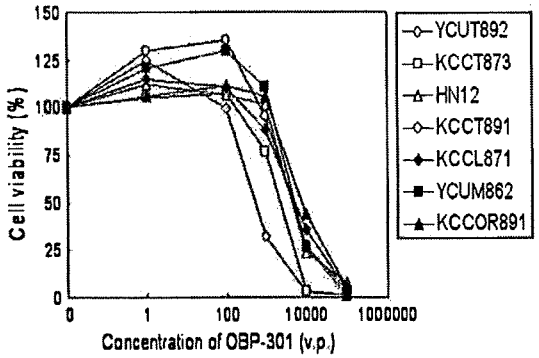

Figure 1. Sensitivity of SCCHN cells to OBP-301 *in vitro*. Cytotoxic activity of OBP-301 on 13 SCCHN cell lines was evaluated by XTT assay. Cells were cultured with various concentrations of OBP-301 (0-100,000 vp/mL). Mean ± SD of quadruplicate determinations. The assay was repeated three times.

the virus to the cell surface through CAR (20). Following attachment, the internalization of the virus into cells occurs through the integrin receptors $\alpha_V\beta_3$ and $\alpha_V\beta_5$ that are expressed in most cell types (19).

Previously, OBP-301 has been reported to induce cell death of human non-small cell lung, colorectal, and prostate cancers *in vitro* and *in vivo* (15, 17). The present study investigates the cytotoxic activity of OBP-301 in 13 SCCHN cell lines and the association between cytotoxic activity and adenoviral receptor expression. We also assessed the *in vivo* antitumor activity and toxicity and tolerability of OBP-301 in an athymic nude mouse model with KCCT873 SCCHN tumors.

Materials and Methods

Adenovirus

The recombinant replication-selective, tumor-specific adenoviral vector OBP-301 was provided by Oncolys Biopharma. The hTERT promoter element drives the expression of *E1A* and *E1B* genes linked with an internal ribosome entry site (15). The virus particle (vp) titer-to-infection titer (plaque-forming units) ratios were 110:3.

Cells

The human non-small cell lung cancer cell line H1299 was cultured in RPMI 1640 supplemented with 10% fetal bovine serum, 1 mmol/L HEPES (Nacalai Tesuque), 100 μg/mL penicillin, and 100 μg/mL streptomycin (Nacalai Tesuque). The SCCHN cell line HN12 was grown in MEM containing 10% fetal bovine serum, 100 μg/mL penicillin, and 100 μg/mL streptomycin. The SCCHN cell lines YCUT892, KCCT873, KCCT891, KCCL871, YCUM862, KCCOR891, YCUL891, YCUM911, YCUMS861, YCUT891, 012SCC, and Wmm-SCC (21) were cultured in RPMI 1640 containing 10% fetal bovine serum, 1 mmol/L HEPES, 100 μg/mL penicillin, and 100 μg/mL streptomycin.

Cell Viability Assay

The XTT assay was done to measure cell viability. Briefly, cells were plated on 96-well plates at 1×10^3 per well 24 h before viral infection. Cells were then infected with 1 to 1×10^5 multiplicity of infection (vp) of OBP-301 and further cultured for 120 h. Cell viability was determined using the Cell Proliferation Kit II (Roche Diagnostics) according to the protocol provided by the manufacturer.

Flow Cytometry

Cells (1×10^5) were labeled with mouse monoclonal anti-CAR (RmcB; Upstate Cell Signaling Solution), anti-integrin $\alpha_V\beta_3$ (Chemicon), anti-integrin $\alpha_V\beta_5$ (Chemicon), or anti-heparan sulfate (Seikagaku) for 60 min at 4°C, incubated with FITC-conjugated goat anti-mouse IgG secondary antibody (Chemicon), and analyzed by the FACSCalibur flow cytometer (Becton Dickinson) using CellQuest software. Control cells were incubated with anti-mouse IgG primary antibody (BD Bioscience) and FITC-conjugated goat anti-mouse IgG secondary antibody. G-means were calculated by the following formula: (G-means of antibody-treated cells) - (G-means of control cells). Correlation coefficients were obtained between the expression levels of CAR, integrin $\alpha_V\beta_3$, integrin $\alpha_V\beta_5$, HSG, and the ID_{50} of OBP-301 in 7 SCCHN cell lines.

Quantitative Real-time PCR Analysis

Total RNA from cultured cells was obtained using the RNeasy Mini kit (Qiagen). Total RNA (~0.1 μg) was used for reverse transcription. Reverse transcription was done at 22°C for 10 min and then at 42°C for 20 min. The *hTERT* mRNA copy number was determined by real-time quantitative reverse transcription-PCR using a LightCycler instrument and a LightCycler DNA TeloTAGGG kit (Roche Diagnostics). PCR amplification was run with activation at 95°C for 15 s, annealing at 58°C for 10 s, and extension at 72°C for 9 s.

Athymic Nude Mouse Models of Human Head and Neck Cancer

Five- to 6-week-old female athymic nude mice (BALB/c *nu/nu*) were obtained from SLC. Animal care was in

Table 1. Cytotoxic activity of adenoviral receptors on head and neck cancer cell lines

Cell line	Origin	ID_{50} (vp)*
YCUT892	Tongue	759
KCCT873	Tongue	4,279
HN12	Lymph node	6,943
KCCT891	Hypopharynx	7,025
YCUM862	Oropharynx	7,512
KCCL871	Larynx	7,599
KCCOR891	Oral floor	9,204
YCUL891	Larynx	ND
YCUM911	Oropharynx	ND
YCUMS861	Maxillary sinus	ND
YCUT891	Tongue	ND
012SCC	Unknown	ND
Wmm-SCC	Unknown	ND

Abbreviation: ND, not done.
*ID_{50}, infection dose of OBP-301 at which 50% inhibition of cell viability is observed compared with untreated cells.

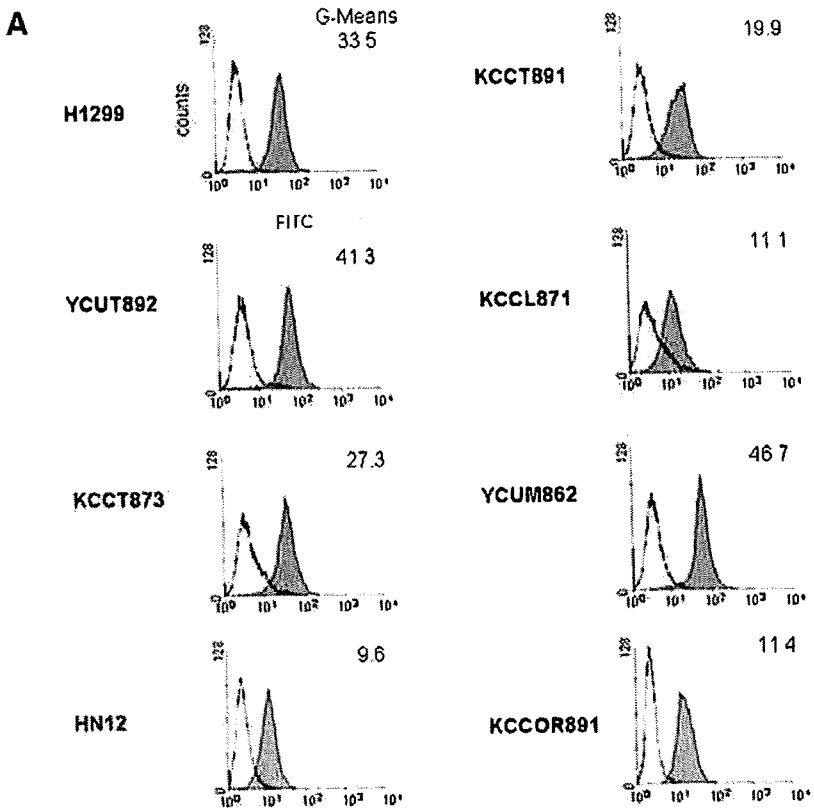

C

Cell line	αVβ3	αVβ5	HSG
H1299	5 16	9 6	27 1
YCUT892	0.5	7 7	102.4
KCCT873	31.1	10.8	9.6
HN12	1.9	4.4	7 0
KCCT891	1.6	5.5	7 7
KCCL871	2 9	4.6	105 4
YCUM862	1.5	1.3	20 7
KCCOR891	2 0	8.8	156 5
correlation coefficient	**-0.2**	**-0.3**	**0.1**

Figure 2. Expression of the CAR in SCCHN cell lines. **A**, cells were incubated with mouse monoclonal anti-CAR (RmcB) followed by detection with FITC-labeled secondary antibody. *Gray histogram*, staining with anti-CAR antibody treatment. H1299 human lung cancer cells were used as a positive control. **B**, correlation between CAR expression in SCCHN cells and the ID_{50} of OBP-301 for these cells. **C**, correlation between integrins $\alpha_V\beta_3$ and $\alpha_V\beta_5$ and HSG expression in SCCHN cells and the ID_{50} of OBP-301 for these cells. The experiment was repeated three times.

accordance with the guidelines of the Kyoto University School of Medicine. A SCCHN model was established in nude mice by s.c. injection of KCCT873 tumor cells (5×10^6) in 150 μL PBS into the flank. Palpable tumors developed within 3 to 4 days. Tumors were measured by vernier calipers. Six to 7 mice were used for each group.

Toxicity Assessment

Blood samples and organs were collected from athymic nude mice at day 10 or 17 after i.t. administration of OBP-301 (3×10^{10} vp/d for days 5-9). Organs from the experimental animals were fixed in 10% formalin, and 5 μm tissue sections were prepared and stained with H&E.

Statistical Analysis

Tumor volume on a given day was calculated by the following formula: (length of the tumor) × (width of the tumor)^2 / 2. The statistical significance of tumor regression was calculated by the Student's *t* test.

Results

Cytotoxic Activity of OBP-301 to Various SCCHN Cell Lines

We first examined the effect of OBP-301 infection on the viability of SCCHN cell lines assessed by the XTT assay.

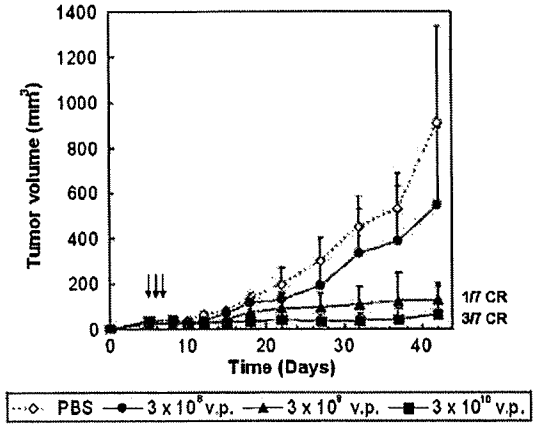

Figure 3. OBP-301 acted in a dose-dependent manner in KCCT873 tumor-bearing mice. Athymic nude mice received s.c. implantation of 5 × 10^6 KCCT873 cells on day 0. Animals then received injections of OBP-301 at the doses of 3 × 10^8 (●), 3 × 10^9 (▲), or 3 × 10^{10} vp (■) on days 5 to 7 (total of three injections). Each group had 7 animals, and the injection volume was 30 μL in each tumor. *Arrows*, day of injections. *Bars*, SD. The experiment was repeated two times.

Because OBP-301 showed slightly cytotoxic activity against 7 of 13 cell lines at a dose of 1,833 vp (50 plaque-forming units/cell), we assessed the ID_{50} of OBP-301 using these 7 SCCHN cell lines (Fig. 1; Table 1). As shown in Table 1, OBP-301 shows modest to strong cytotoxic activity in the 7 cell lines tested, with the ID_{50} varying from 759 to 9,204 vp. The cytotoxic activity of OBP-301 in these cell lines shows dose dependence (Fig. 1). YCUT892 cells were most sensitive to OBP-301 followed by KCCT873, HN12, KCCT891, YCUM862, KCCL871, and KCCOR871 cells, suggesting that 2 of the SCCHN cell lines are most sensitive to OBP-301.

Expression of Adenovirus Receptors in SCCHN Cell Lines

Because the cytotoxic activity of OBP-301 was anticipated to be correlated with efficiency of adenoviral infection through CAR, integrin $\alpha_V\beta_3$, integrin $\alpha_V\beta_5$, or HSG receptors (22), we then assessed the expression levels of CAR on SCCHN cells using flow cytometry. As shown in Fig. 2A, all 7 SCCHN cell lines have been found to express detectable levels of CAR. However, as shown in Fig. 2B, correlation between the cytotoxic activity of OBP-301 and the expression level of CAR was not significant (correlation coefficient = −0.5). In addition, we assessed the expression of integrin $\alpha_V\beta_3$, integrin $\alpha_V\beta_5$, and HSG in SCCHN cell lines; however, the expression levels were not correlated with cytotoxic activity of OBP-301 (Fig. 2C). We also assessed *hTERT* expression using the quantitative PCR method and found that all of the SCCHN cell lines express detectable levels of *hTERT* mRNA; however, there was no correlation between the expression levels and ID_{50} of OBP-301 in these cells (data not shown). These results suggest that, although 7 of 13 SCCHN cell lines are sensitive to OBP-301, its ability to enter the cell is not necessarily correlated with the degree of cytotoxicity.

Antitumor Effect of OBP-301 in SCCHN-Bearing Animals

To assess the antitumor effect of OBP-301 in the animal model of human SCCHN, KCCT873 cells were implanted s.c. in athymic nude mice (6, 23) to examine the effect of OBP-301 at a variety of dosages *in vivo*. Mice received i.t. injections of OBP-301 at 3 × 10^8, 3 × 10^9, or 3 × 10^{10} vp for 3 days from days 5 to 7 after tumor implantation (Fig. 3). Tumors grew to mean tumor volume of 32.2 ± 4.5 mm^3 at day 5. As shown in Fig. 3, the 3 × 10^8 dose of OBP-301 treatment was less effective against KCCT873 tumor growth. The mean tumor volume was 549 mm^3 on day 42, which is comparable with control tumor volume (910 mm^3). Higher doses of OBP-301 led to superior antitumor activity. The mean tumor volume of treated tumors was 130 mm^3 at 3 × 10^9 vp and 67 mm^3 at 3 × 10^{10} vp, which is significantly smaller compared with the control tumor at day 42 ($P < 0.0001$). Remarkably, in addition to a 93% inhibition in tumor volume in mice receiving a 3 × 10^{10} vp dosage, 3 of 7 tumors completely disappeared by day 37, which persisted through day 42. These results suggest that OBP-301 shows a remarkable antitumor effect in a dose-dependent manner in KCCT873 SCCHN tumors. Based on these findings, OBP-301 at a dosage of 3 × 10^{10} vp per injection shows the maximum tumor reduction effect.

Optimization of OBP-301 Injection Times in KCCT873 SCCHN Tumors

We next evaluated the treatment schedule of OBP-301 in s.c. xenografted KCCT873 tumor-bearing mice. Mice were treated i.t. with OBP-301 for 1, 3, or 5 subsequent days. The

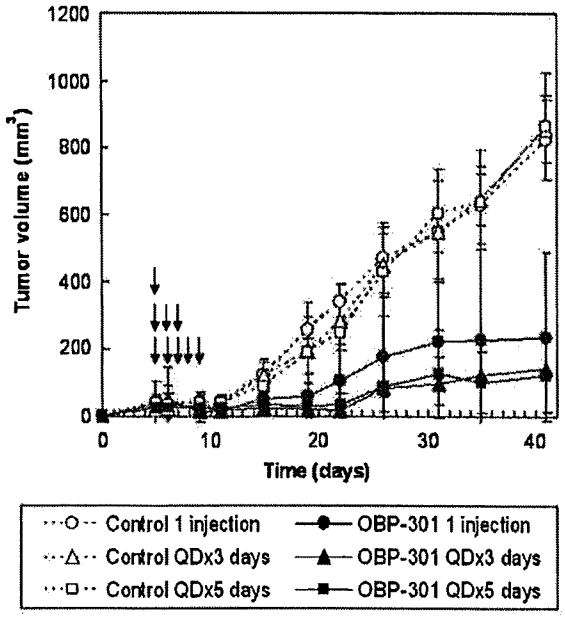

Figure 4. Regression of KCCT873 tumors by i.t. treatment of OBP-301. Athymic nude mice receiving s.c. KCCT873 implantation were treated with OBP-301 (3 × 10^{10} vp) for 1 (●), 3 (▲), or 5 (■) days. Injections were made on consecutive days (*QD*). Each group had 6 animals, and the injection volume was 30 μL in each tumor. *Arrows*, day of injections. *Bars*, SD. The experiment was repeated two times.

OBP-301 treatment started on day 5 (mean tumor volume, 31.4 ± 7.3 mm^3), as palpable tumors developed within 3 to 4 days. As shown in Fig. 4, i.t. administration of OBP-301 showed considerable antitumor activity in all groups. The mean tumor volume of animals receiving a one-time injection was 236 mm^3 at day 41, 71% smaller than excipient-only injected control tumors (823 mm^3; $P < 0.0001$). Interestingly, three or five injections of OBP-301 treatment showed superior antitumor activity. The mean tumor volume of animals in the group receiving a three-time treatment was 142 mm^3 at day 41, 83% smaller than control tumors (856 mm^3; $P < 0.0001$). Three of 6 tumors had completely regressed by day 27; however, later on, all of the tumors appeared and slowly started to grow again by day 41. Animals receiving OBP-301 for 5 days showed superior tumor response, including complete disappearance of tumors in 2 of 6 mice through day 41. The mean tumor volume measured on day 41 (121 mm^3) was 86% smaller than control tumors (863 mm^3; $P < 0.0001$). These results suggest that three- and five-time injections of OBP-301 treatment were equally effective in KCCT873 SCCHN tumor reduction.

Toxicity Profile in Mice Treated with OBP-301

Finally, to assess the toxicity and safety profile of OBP-301 treatment, blood and major organs including heart, liver, lung, kidney, and spleen were collected from KCCT873 tumor-bearing athymic nude mice receiving i.t. OBP-301 (3×10^{10} vp/d for 5 days) on day 10 or 17 after tumor implantation. As shown in Table 2, a blood serum chemistry analysis showed no remarkable changes in any variable in all the mice tested, except for a minor elevation of creatinine phosphokinase and aspartate aminotransferase in the OBP-301 treatment group. Similarly, no pathologic alterations were observed in any of the organs tested (data not shown). Although a slight necrosis was observed in livers from mice treated with i.t. OBP-301, all other organs from untreated control and OBP-301-treated mice did not show any evidence of toxicity. The result that all the treated mice tolerated therapy very well without any behavioral changes or toxicities in blood and pathology suggests that OBP-301 treatment leads to considerable antitumor activity without unwanted safety or toxicity issues.

Discussion

Although it has been reported that OBP-301 showed a strong anticancer activity in colorectal, prostate, and non-small cell lung cancer *in vitro* and *in vivo*, the effect of OBP-301 in SCCHN has not been pursued (17, 18, 24). Therefore, in this study, we planned to assess the detailed antitumor and toxicity profile of OBP-301 in an animal model of SCCHN. OBP-301 induces cell death in 7 of 13 cell lines *in vitro* and shows dramatic antitumor effects in an animal model bearing KCCT873 tumors without significant toxicity.

OBP-301 showed cytotoxic activity in 7 of 13 SCCHN cell lines. Because the effect of OBP-301 against SCCHN cell lines was limited compared with that previously shown against human non-small cell lung, colorectal, and prostate cancer cell lines (14, 17), we hypothesized that the limitation came from the lower viral infection rate. However, it is of interest to note that the expression levels of adenoviral receptors including CAR, integrins, and HSG are comparable between SCCHN and non-small cell lung cancer H1299 cell lines (Fig. 2; data not shown). In addition, we did not find a significant correlation between *hTERT* mRNA expression and the cytotoxic activity of OBP-301. These results suggest that various factors such as replication speed of viruses and the existence of unknown receptors might be involved in the cytotoxic activity of OBP-301.

The i.t. three- or five-time administration of OBP-301 dramatically inhibited the growth of KCCT873 tumors *in vivo*. The antitumor effect was actually superior to what we expected from our *in vitro* results. Previously, we reported that adenovirus present in blood of mice exists for at least 1 week after i.t. treatment with OBP-301 (15, 17), and i.t. OBP-301 showed antitumor effects both in the injected primary tumor site and in tumors located at distant sites (17). From these results, it is conceivable that OBP-301 attacked the xenografted KCCT873 tumor over and over through the bloodstream for at least 1 week after injection.

Table 2. Changes in blood serum chemistry of mice receiving OBP-301 treatment

Profile	Untreated control	Day 10*		Day 17*	
		PBS	OBP-301	PBS	OBP-301
Sodium (mEq/L)	156	153	151	157	156
Potassium (mEq/L)	7.5	7.3	9.3	8.7	8.2
Creatinine phosphokinase (units/L)	4,007	6,895	8,790	4,907	6,508
Lactate dehydrogenase (units/L)	2,153	3,197	3,158	2,600	2,740
Aspartate aminotransferase (units/L)	195	274	445	349	536
Alanine aminotransferase (units/L)	38	48	64	62	71
Bilirubin (mg/dL)	0.1	0.1	0.1	0.1	0.1
Creatinine (mg/dL)	0.16	0.13	0.13	0.14	0.13

NOTE: Data are mean blood samples from 3 animals in each group.
*Blood samples were collected from athymic nude mice receiving five i.t. injections of OBP-301 (days 5-9).

It has been reported that oncolytic virus replication induces tumor-specific immune responses by stimulating uric acid production as a danger signal as well as accelerating tumor antigen cleaved by IFN-γ-inducible PA28 expression (18). Additionally, because it has been shown that telomerase is active in ~80% to 90% of SCCHN tumor tissues as assessed by immunohistochemistry (25), we speculate that SCCHN cancer preferentially responds to OBP-301 treatment. These results may be the reason why the antitumor activity of OBP-301 is more profound in KCCT873 tumors than expected from our *in vitro* results. Therefore, the strong anticancer effect shown in these animal studies suggests that OBP-301 could be an attractive agent to accomplish an *in situ* radical cure of SCCHN patients.

Although chemoradiotherapy, radiotherapy plus concurrent chemotherapy, has become the standard care for patients with unresectable SCCHN and organ preservation (26, 27), it has recently been reported that cisplatin and fluorouracil with docetaxel plus chemoradiotherapy has a greater effect (28). Because our previous study showed that OBP-401 containing a green fluorescent protein gene for monitoring viral replication (TelomeScan) showed enhanced antitumor efficacy in an *in vivo* human lung cancer model when given in combination with docetaxel, it is possible that combination of OBP-301 with conventional chemotherapy may be a powerful regimen for the treatment of SCCHN in the clinic (29). Additionally, as SCCHN is easily acceptable site for direct injection (6) and i.t. OBP-301 was emerged strong antitumor effect in the xenografted KCCT873 tumor, the i.t. OBP-301 may be a new tool for the treatment of head and neck cancer. Future directions of clinical exploration with OBP-301 are still being considered. Utilization of OBP-301 via i.t. injection appears to be associated with modest activity, although clinical utility of local regional therapy is limited. Further exploration via intrahepatic arterial infusion or i.v. infusion awaits discovery of methods to improve OBP-301 activity.

Viral replication generally results in tissue destruction. In fact, interactions between adenovirus type 5 with CAR, integrin $\alpha_V\beta_3$, integrin $\alpha_V\beta_5$, or HSG and the fiber shaft of adenovirus type 5 are known to be involved in accumulation in the liver of mice and cynomolgus monkeys when administered (30–33). In this study, a significant therapeutic effect of i.t. OBP-301 treatment was achieved without any significant liver toxicity. Histologic analyses in the brain, lung, heart, kidney, and spleen showed no toxicity profile. Oncolytic viruses have been developed as anticancer agents because controlled replication in the tumors causes selective killing of tumor cells and minimizes the effect on normal cells (34). Thus, the current results are consistent with the mechanism of action of virotherapy with oncolytic viruses.

Notably, a phase I study of OBP-301 has been initiated in the United States to test the safety and tolerability of OBP-301 in patients with various types of progressive solid cancer including SCCHN. Results from current clinical trials may further show additional information on its safety and efficacy. As for the clinical use of OBP-301 in SCCHN, the preliminary information obtained from our study is, based on the present results, considered to be useful for the planning of future clinical trials.

In conclusion, this study clearly shows that OBP-301 has remarkable *in vivo* anticancer effects against SCCHN. These findings suggest that the replication-selective oncolytic virus provides a new platform for treating patients with human head and neck cancer.

Disclosure of Potential Conflicts of Interest

Y. Urata and D. Ichimaru: employees of Oncolys Biopharma Inc. T. Fujiwara: consultant to Oncolys Biopharma Inc. No other potential conflicts of interest were disclosed.

Acknowledgments

We thank Dr. Hisashi Urushihara and Ritsuko Asai for technical support.

References

1. Jemal A, Siegel R, Ward E, et al. Cancer statistics, 2006. CA Cancer J Clin 2006;56:106–30.

2. Argiris A, Karamouzis MV, Raben D, et al. Long-term results of a phase III randomized trial of postoperative radiotherapy with or without carboplatin in patients with high-risk head and neck cancer. Laryngoscope 2008;118:444–9.

3. Cohen EE, Lingen MW, Vokes EE. The expanding role of systemic therapy in head and neck cancer. J Clin Oncol 2004;22:1743–52.

4. Coevas AD. Chemotherapy options for patients with metastatic or recurrent squamous cell carcinoma of head and neck. J Clin Oncol 2006; 24:2644–52.

5. Karamouzis MV, Argiris A, Grandis JR. Clinical applications of gene therapy in head and neck cancer. Curr Gene Ther 2007;7:446–57.

6. Kawakami K, Kawakami M, Joshi BH, Puri RK. Interleukin-13 receptor-targeted cancer therapy in an immunodeficient animal model of human head and neck cancer. Cancer Res 2001;61:6194–200.

7. Blackburn EH. Structure and function of telomeres. Nature (Lond) 1991;350:569–73.

8. Kim NW, Piatyszek MA, Prowse KR, et al. Specific association of human telomerase activity with immortal cells and cancer. Science 1994; 266:2011–5.

9. Shay JW, Wright WE. Telomerase activity in human cancer. Curr Opin Oncol 1996;8:66–71.

10. Nakayama J, Tahara H, Tahara E, et al. Telomerase activation by hTERT in human normal fibroblasts and hepatocellular carcinomas. Nat Genet 1998;18:65–8.

11. Bischoff JR, Kirn DH, Williams A, et al. An adenovirus mutant that replicates selectively in p53-deficient human tumor cells. Science 1996; 274:373–6.

12. Rodriguez R, Schuur ER, Lim HY, Henderson GA, Simons JW, Henderson DR. Prostate attenuated replication competent adenovirus (ARCA) CN706: a selective cytotoxic for prostate-specific antigen-positive prostate cancer cells. Cancer Res 1997;57:2559–63.

13. Tsukuda K, Wiewrodt R, Molnar-Kimber K, Jovanovic VP, Amin KM. An E2F-responsive replication-selective adenovirus targeted to the defective cell cycle in cancer cells: potent antitumoral efficacy but no toxicity to normal cell. Cancer Res 2002;62:3438–47.

14. Li Y, Yu DC, Chen Y, et al. A hepatocellular carcinoma-specific adenovirus variant, CV890, eliminates distant human liver tumors in combination with doxorubicin. Cancer Res 2001;61:6428–36.

15. Kawashima T, Kagawa S, Kobayashi N, et al. Telomerase-specific replication-selective virotherapy for human cancer. Clin Cancer Res 2004; 10:285–92.

16. Umeoka T, Kawashima T, Kagawa S, et al. Visualization of intrathoracically disseminated solid tumors in mice with optical imaging by telomerase-specific amplification of a transferred green fluorescent protein gene. Cancer Res 2004;64:6259–665.

17. Huang P, Watanabe M, Kaku H, et al. Direct and distant antitumor

effects of a telomerase-selective oncolytic adenoviral agent, OBP-301, in a mouse prostate cancer model. Cancer Gene Ther 2008;15:315–22.

18. Endo Y, Sakai R, Ouchi M, et al. Virus-mediated oncolysis induces danger signal and stimulates cytotoxic T-lymphocyte activity via proteasome activator upregulation. Oncogene 2008;27:2375–81.

19. Wickham TJ, Mathias P, Cheresh DA, Nemerow GR. Integrins $\alpha_v\beta_3$ and $\alpha_v\beta_5$ promote adenovirus internalization but not virus attachment. Cell 1993;73:309–19.

20. Bergelson JM, Cunningham JA, Droguett G, et al. Isolation of a common receptor for coxsackie B viruses and adenoviruses 2 and 5. Science 1997;275:1320–3.

21. Kawakami K, Leland P, Puri RK. Structure, function, and targeting of interleukin 4 receptors on human head and neck cancer cells. Cancer Res 2000;60:2981–7.

22. Koizumi N, Kawabata K, Sakurai F, Watanabe Y, Hayakawa T, Mizuguchi H. Modified adenoviral vectors ablated for coxsackievirus-adenovirus receptor, α_v integrin, and heparan sulfate binding reduce *in vivo* tissue transduction and toxicity. Hum Gene Ther 2006;17:264–79.

23. Ishii KJ, Kawakami K, Gursel I, et al. Antitumor therapy with bacterial DNA and toxin: complete regression of established tumor induced by liposomal CpG oligodeoxynucleotides plus interleukin-13 cytotoxin. Clin Cancer Res 2003;9:6516–22.

24. Watanabe T, Hioki M, Fujiwara T, et al. Histone deacetylase inhibitor FR901228 enhances the antitumor effect of telomerase-specific replication-selective adenoviral agent OBP-301 in human lung cancer cells. Exp Cell Res 2006;312:256–65.

25. Mao L, El-Naggar AK, Fan YH, et al. Telomerase activity in head and neck squamous cell carcinoma and adjacent tissues. Cancer Res 1996;56:5600–4.

26. Denis F, Garaud P, Bardet E, et al. Final results of the 94-01 French Head and Neck Oncology and Radiotherapy Group randomized trial comparing radiotherapy alone with concomitant radiochemotherapy in advanced-stage oropharynx carcinoma. J Clin Oncol 2004;22:69–76.

27. Forastiere AA, Goepfert H, Maor M, et al. Concurrent chemotherapy and radiotherapy for organ preservation in advanced laryngeal cancer. N Engl J Med 2003;349:2091–8.

28. Posner MR, Hershock DM, Blajman CR, et al. Cisplatin and fluorouracil alone or with docetaxel in head and neck cancer. N Engl J Med 2007;357:1705–15.

29. Fujiwara T, Kagawa S, Kishimoto H, et al. Enhanced antitumor efficacy of telomerase-selective oncolytic adenoviral agent OBP-401 with docetaxel: preclinical evaluation of chemovirotherapy. Int J Cancer 2006;119:432–40.

30. Nakamura T, Sato K, Hamada H. Reduction of natural adenovirus tropism to the liver by both ablation of fiber-coxsackievirus and adenovirus receptor interaction and use of replaceable short fiber. J Virol 2003;77:2512–21.

31. Smith TA, Idamakanti N, Rollence ML, et al. Adenovirus serotype 5 fiber shaft influences *in vivo* gene transfer in mice. Hum Gene Ther 2003;14:777–87.

32. Smith TA, Idamakanti N, Marshall-Neff J, et al. Receptor interactions involved in adenoviral-mediated gene delivery after systemic administration in non-human primates. Hum Gene Ther 2003;14:1595–604.

33. Vigne E, Dedieu JF, Brie A, et al. Genetic manipulations of adenovirus type 5 fiber resulting in liver tropism attenuation. Gene Ther 2003;10:153–62.

34. Kirn D, Martuza RL, Zwiebel J. Replication-selective virotherapy for cancer: biological principles, risk management and future directions. Nat Med 2001;7:781–7.

Invest New Drugs (2009) 27:241–245
DOI 10.1007/s10637-008-9169-5

PRECLINICAL STUDIES

Antiviral activity of cidofovir against telomerase-specific replication-selective oncolytic adenovirus, OBP-301 (Telomelysin)

Masaaki Ouchi · Hitoshi Kawamura · Yasuo Urata · Toshiyoshi Fujiwara

Received: 15 June 2008 / Accepted: 30 July 2008 / Published online: 27 August 2008

Summary We constructed a replication-competent oncolytic adenovirus, OBP-301 (Telomelysin), in which human telomerase reverse transcriptase (hTERT) promoter drives E1 genes. OBP-301 is currently being used in a phase-I clinical trial for various types of tumors. Under such conditions, anti-adenoviral agents should be available for safety use against OBP-301 since any adenoviral viremia could cause severe adverse effects. Cidofovir (CDV) is an acyclic nucleoside phosphonate that has a broad antiviral activity against DNA viruses. Here, we examined the antiviral effects of CDV against OBP-301. The *in vitro* cytopathic effects of OBP-301 were suppressed by CDV. Moreover, CDV decreased the adenoviral E1A gene copy number after OBP-301 infection. These results suggest that CDV is a potentially useful antiviral agent for OBP-301.

Keywords hTERT · Adenovirus · Cidofovir · Oncolytic virus · Clinical trial

Introduction

Oncolytic adenoviruses have been developed for treatment of human cancer. These viruses are designed to replicate and selectively kill cancer cells but to have minimum effect on normal cells [1]. Two major approaches to generate selective replication of viruses within tumor cells have been used [2, 3]. One is to delete genes that are critical for replication of the virus in normal cells but are dispensable for cancer cells such as ONYX-015 or Δ24 [4]. The other approach is the replacement of the promoter region that initiates viral replication genes to the promoter region of the genes active in cancer cells [2, 3]. Various genetic or epigenetic targets limited to cancer cells have been investigated and used for constructing oncolytic adenoviruses.

Human telomerase reverse transcriptase (hTERT) is an enzymatic subunit of human telomerase [5]. Telomerase is expressed in almost all cancer cells but not in all normal cells [6]. Therefore, telomerase is an attractive target for treatment of cancer. We constructed previously the attenuated adenovirus, OBP-301 (Telomelysin), in which adenoviral E1A and E1B genes are linked with internal ribosomal entry site under the control of the hTERT promoter. We reported that OBP-301 induced selective expression of E1A and E1B genes in many cancer cell lines and selectively replicated and lysed cancer cells but not normal cells [7–9]. OBP-301 is currently being tested in a phase-I clinical trial that includes various types of solid tumors. Although patients receiving this type of therapy become positive for anti-adenoviral neutralizing antibodies, those treated with OBP-301 could develop adenoviral viremia with potentially severe adverse effects. Thus, there is a need for anti-adenoviral agents for treatment of potential viremia in clinical trials of OBP-301.

One of the antiviral compounds is phosphonyl acyclic nucleotides, (S)-9-(3-hydroxy-2-phosphonometoxy propyl) cytosine dehydrate, also known as HPMPC (cidofovir, or CDV). CDV was developed for the treatment of viral infections and has a broad antiviral activity against DNA viruses, such as cytomegalovirus and adenoviruses (AdV). CDV exhibits potent inhibitory effects against several

M. Ouchi · H. Kawamura · Y. Urata
Oncolys BioPharma, Inc.,
Tokyo 106-0032, Japan

T. Fujiwara (✉)
Center for Gene and Cell Therapy, Okayama University Hospital,
Okayama 700-8558, Japan
e-mail: toshi_f@md.okayama-u.ac.jp

adenoviral serotypes in cell culture models [10]. Furthermore, CDV has been used clinically for AdV infections after bone marrow transplantation in immunodeficient patients [11]. Thus, we presumed that CDV could be a useful antiviral drug against OBP-301. In the present study, we examined the *in vitro* inhibitory effects of CDV against OBP-301 in human lung cancer cell lines.

Materials and methods

Cell culture, viruses, and chemicals

The human non-small lung cancer cell H1299 and lung cancer cell line A549 were purchased from American Type Culture Collection (ATCC). H1299 was cultured in RPMI 1640 medium supplemented with 10% FCS. A549 was cultured in DMEM F12 medium supplemented with 10% fetal calf serum (FCS). OBP-301 was constructed and characterized as described previously [7-9]. The human wild-type adenovirus type 5 (wt-Ad) was also used. VISTIDE™ (CDV injection) was purchased from Gilead Sciences (Foster City, CA).

Cell viability assay

Cells were seeded in 96-well plate at 1×10^3 cells per well and incubated at 37°C. After incubation, cells were infected with OBP-301 at a MOI of 1 (in H1299) and 5 (in A549) for 2 hours. The medium was aspirated and replaced with fresh medium containing 2% FCS and serially diluted CDV. Cell viability was determined by XTT assay 7 days after infection using Cell Proliferation Kit II (Roche Molecular Biochemicals) according to the protocol recommended by the manufacturer. Protection was determined by the following formula: Protection (%)={OD (AdV(+):CDV (+)) − OD (AdV (+):CDV(−))}/{OD (AdV(−):CDV(+)) −OD (AdV (+):CDV(−))}×100. CC_{50} (50% cytotoxic concentration) was defined as CDV concentration that inhibited relative cell viability to 0.5 without OBP-301 infection. EC_{50} (50% effective concentration) was defined as CDV concentration that archived 50% protection.

Quantitative real-time PCR analysis

Cells were seeded in six-well plate at 2×10^5 cells per well. After overnight incubation at 37°C, the medium was aspirated, and cells were infected with OBP-301 or wt-Ad at a MOI of 10 for 2 hours at 37°C with gentle shaking every 15 minutes. After incubation, the cells were washed with PBS and placed in a medium containing serially diluted CDV (100, 20, 4, 0.8, 0.16 and 0 μM). The cells were harvested 24 hours later with Trypsin/EDTA and total DNA was extracted using QIAamp™ DNA Mini Kit (Qiagen, Hilden, Germany). Viral E1A copy number was measured using LightCycler instruments and LightCycler Faststart DNAMaster SYBR Green 1 (Roche, Mannheim, Germany). EC_{50} (E1A) was defined as the CDV concentration that inhibits the E1A ratio (with CDV/no CDV) to 0.5. Primers for E1A gene were: forward: 5'- CCTGTGTCTA GAGAATGCAA -3', reverse: 5'- ACAGCTCAAGTC CAAAGGTT - 3'. PCR amplification began with a 600-s of denaturation step at 95°C and then 40 cycles of denaturation at 95°C for 10 s, annealing at 60°C for 15 s, and extension at 72°C for 8 s.

Statistical analysis

The Student's *t*-test was used to compare differences. Statistical significance was defined when p was <0.05.

Results

In vitro cytopathic effect of OBP-301 on lung cancer cell lines

We reported previously that OBP-301 exhibited oncolytic activity against many types of human cancer cells [7–9]. To confirm this, we tested its cytopathic effects in cancer cell line *in vitro*. Human lung cancer cell lines, A549 and H1299, were infected with OBP-301 at various MOIs and numbers of living cells were measured by XTT assay (Fig. 1). At 5 days after infection, the majority of H1299 cells were killed by OBP-301 at MOI of 1 and 10, and approximately 70% of A549 cells were killed by OBP-301 at MOI of 50. These results confirmed that OBP-301 induced cell death in A549 and H1299 cells.

Inhibitory effects of CDV on the cytopathic effect of OBP-301

Next, we tested whether the cytopathic effect by OBP-301 on these cancer cells could be inhibited by CDV treatment. A549 and H1299 cells were infected with OBP-301 then treated with CDV at various concentrations. Cell viability was also determined by XTT assay. In the presence of the drug and virus, relative cell viability significantly increased in the presence of CDV at > 30 μM in A549 cells and > 40 μM in H1299 cells ($p<0.01$) (Fig. 2). Furthermore, inhibition of cell growth of each cell line was observed in the presence of CDV at > 100 μM. The calculated EC_{50} values of CDV were 20.4 μM for H1299 and 35.9 μM for A549 cells, while the calculated CC_{50} values were 146.4 μM for H1299 cells and 106.9 μM for A549 cells. Similar results were obtained by using ONYX-015 (see

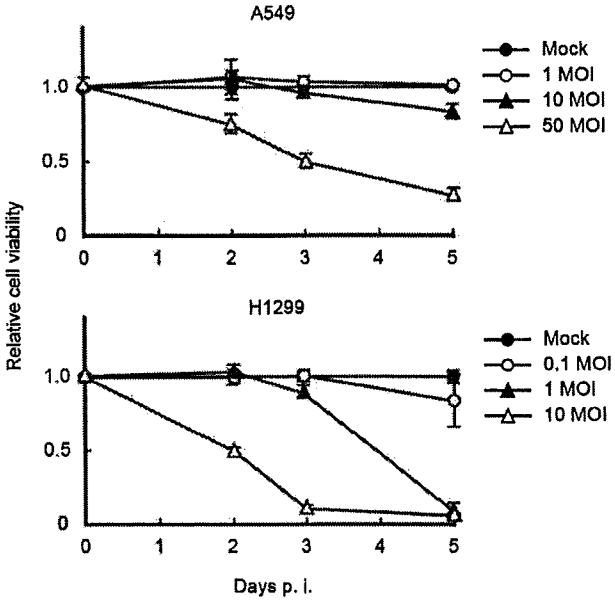

Fig. 1 Cytopathic effects of OBP-301 on H1299 and A549 lung cancer cell lines *in vitro*. Each cell was infected with OBP-301 at the indicated MOI and cell viability was evaluated by XTT assay (no virus=1.0). Data are mean±SD values

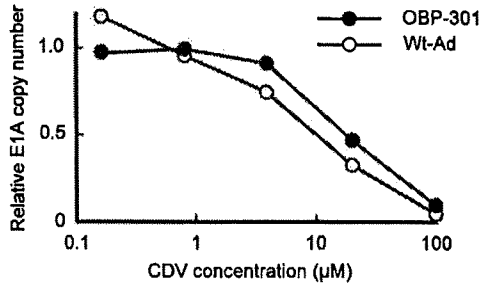

Fig. 3 Inhibition of OBP-301 replication in H1299 cells by CDV. Cells were infected with OBP-301 or wild-type AdV at MOI of 10, followed by the addition of CDV at the indicated concentrations. Cells were collected after 24 hours infection, total DNA was extracted, and viral E1A copy number was determined by quantitative real-time PCR analysis (with virus/no CDV=1.0)

Introduction) and OBP-401, a modified OBP-301 that contains the GFP gene [12] (data not shown).

Inhibitory effects of CDV on viral replication of OBP-301

Finally, we examined whether CDV inhibits the replication of OBP-301 *in vitro*. We previously used two methods to quantify viral replication, biological plaque forming assay using 293 cells [7] and real-time PCR assay targeting adenoviral E1A sequence [8, 9], and found that both assays could detect viral replication similarly. H1299 cells were infected with OBP-301 or wt-Ad, followed by treatment with CDV. Wt-Ad was used for positive control in this assay since it had been reported that CDV had antiviral activity against wt-Ad. To measure the viral DNA, we quantified E1A copy number of cells infected with OBP-301 or wt-Ad by real-time PCR assay. CDV reduced the relative E1A copy number in both wt-Ad and OBP-301-infected cells and the effect was concentration-dependent, indicating that CDV inhibited viral replication of OBP-301 and wt-Ad in H1299 cells (Fig. 3). The calculated EC_{50} (E1A) value for OBP-301 was 19.55 μM.

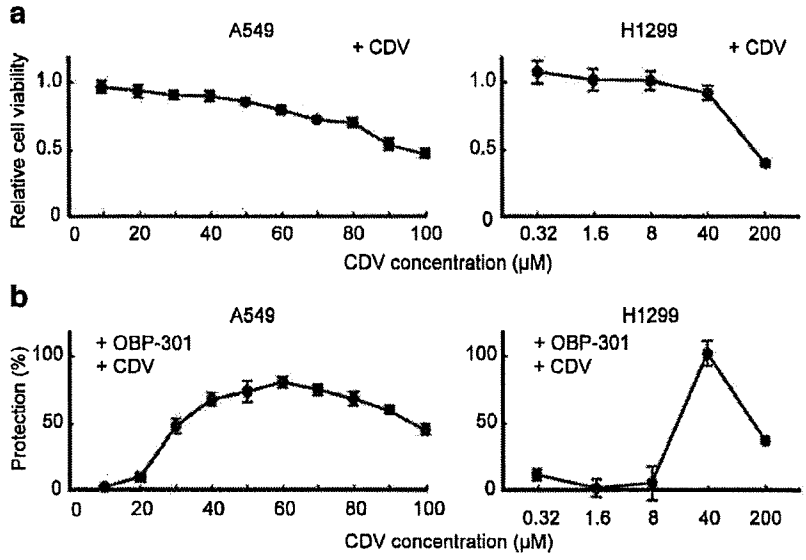

Fig. 2 Inhibition of cytopathic effects of OBP-301 by CDV in human lung cancer cell lines. (**a**) Cells were treated with CDV at the indicated concentrations and incubated for 7 days. The relative cell viability was evaluated by XTT assay. Data are mean±SD values. (**b**) Cells were infected with OBP-301 (1 MOI in H1299 and 5 MOI in A549, PFU/cell), followed by the addition of CDV at the indicated concentrations. Protection was calculated as described in "Material and methods". Data are mean±SD values

Discussion

OBP-301 has been developed as an oncolytic viral agent for the treatment of human cancer and is currently used in a phase-I clinical trial. Although replication of OBP-301 is limited in normal cells evaluated *in vitro* and *in vivo* mouse model, the effect of OBP-301 in human is still unknown. In the phase-II clinical trial of ONYX-015, an E1B-55 kDa-deleted adenovirus mutant, adenoviral viremia occurred even in the presence of neutralizing antibodies and antiviral cytokines [13]. Several antiviral drugs are used for other DNA viruses, e.g. aciclovir, a synthetic acyclic purine-nucleoside analogue, for Herpes simplex virus (HSV) [14], and ganciclovir (GCV) for Cytomegalovirus infections [15]. For AdV infections, it has been reported that CDV exhibits potent inhibitory effects against several adenoviral serotypes in cell culture models [10, 16]. We considered that CDV can be used as antiviral drug for OBP-301.

The purpose of using CDV clinically is to avoid toxic effects of OBP-301 in normal tissues, when viral replication becomes uncontrollable. However, it is difficult to examine the inhibitory effect of CDV on cytopathic effect of OBP-301 in normal cells, because OBP-301 replicates and lyses only in cancer cells [7–9]. Therefore, we used human cancer cell lines to assess the potential antiviral activity of CDV. We showed that the cytopathic effects of OBP-301 were efficiently suppressed by CDV treatment at concentrations that did not affect cell growth (Fig. 2). Despite the high susceptibility of H1299 cells to OBP-301 infection (Fig. 1), CDV inhibited the cytopathic effects of OBP-301, suggesting that CDV has potent antiviral activity against OBP-301. The 50% effective concentration of CDV in A549 cells was in agreement with the published data using human wt-Ad [17], indicating that the inhibitory activity against the cytopathic effect of OBP-301 was equivalent to that of wt-Ad.

The mechanism of the antiviral effect of CDV is that of inhibition of viral replication by targeting the viral DNA polymerase [18]. The anti-adenoviral effect of CDV is quantified by evaluating the viral progeny in adenovirus-infected cells using quantitative PCR analysis [16]. We demonstrated that the replication of OBP-301 was inhibited by CDV in a concentration-dependent manner (Fig. 3). In addition, the 50% effective concentration on viral DNA copy number was almost the same as the 50% effective concentration on cell death by OBP-301 infection, suggesting that CDV inhibited the cytopathic effect of OBP-301 by inhibiting the replication of OBP-301. Recently, antiviral effect of CDV against wt-Ad in immunosuppressed Syrian hamster model was reported [19]. The 50% inhibitory concentration of CDV on viral DNA copy number in OBP-301 was slightly higher than that of wt-Ad (Fig. 3). Differences at E1A region between OBP-301 and wt-Ad may affect of CDV activity on viral replication. It has been reported that CDV-resistant human Ad mutants were isolated by continuous passage *in vitro* condition [20]. Quality assurance and quality control of the master virus bank have been intensively performed for OBP-301 used in the current clinical trials; emergence of CDV-resistant OBP-301 variant, however, should be considered and long-term susceptibility of CDV against OBP-301 will be studied in the future clinical trials.

In conclusion, our *in vitro* data indicate that CDV can effectively inhibit the oncolytic activity of OBP-301 by inhibiting the replication of OBP-301. CDV may be a potential antiviral agent for OBP-301 in clinical trial.

References

1. Kim D, Martuza RL, Zwiebel J (2001) Replication-selective virotherapy for cancer: biological principles, risk management and future directions. Nat Med 7:781–787. doi:10.1038/89901
2. Kim D (2000) Replication-selective oncolytic adenoviruses: virotherapy aimed at genetic targets in cancer. Oncogene 19:6660–6669. doi:10.1038/sj.onc.1204094
3. Chu RL, Post DE, Khuri FR, Van Meir EG (2004) Use of replicating oncolytic adenoviruses in combination therapy for cancer. Clin Cancer Res 10:5299–5312. doi:10.1158/1078-0432.CCR-0349-03
4. Davis JJ, Fang B (2005) Oncolytic virotherapy for cancer treatment: challenges and solutions. J Gene Med 7:1380–1389. doi:10.1002/jgm.800
5. Nakamura TM, Morfin GB, Chapman KB, Weinrich SL, Andrews WH, Lingner J et al (1997) Telomerase catalytic subunit homologs from fission yeast and human. Science 277:955–959. doi:10.1126/science.277.5328.955
6. Kim NW, Piatyszek MA, Prowse KR, Harley CB, West MD, Ho PL et al (1994) Specific association of human telomerase activity with immortal cells and cancer. Science 266:2011–2015. doi:10.1126/science.7605428
7. Kawashima T, Kagawa S, Kobayashi N, Shirakiya Y, Umeoka T, Teraishi F et al (2004) Telomerase-specific replication-selective virotherapy for human cancer. Clin Cancer Res 10:285–292. doi:10.1158/1078-0432.CCR-1075-3
8. Taki M, Kagawa S, Nishizaki M, Mizuguchi H, Hayakawa T, Kyo S et al (2005) Enhanced oncolysis by a tropism-modified telomerase-specific replication-selective adenoviral agent OBP-405 (Telomelysin-RGD). Oncogene 24:3130–3140. doi:10.1038/sj.onc.1208460
9. Hashimoto Y, Watanabe Y, Shirakiya Y, Uno F, Kagawa S, Kawamura H et al (2008) Establishment of biological and pharmacokinetic assays of telomerase-specific replication-selective adenovirus. Cancer Sci 99:385–390. doi:10.1111/j.1349-7006.2007.00665.x
10. Gordon YJ, Romanowski E, Araullo-Cruz T, Seaberg L, Erzurum S, Tolman R et al (1991) Inhibitory effect of (S)-HPMPC, (S)-HPMPA, and 2'¢-nor-cyclic GMP on clinical ocular adenoviral isolates is serotype-dependent in vitro. Antivir Res 16:11–16. doi:10.1016/0166-3542(91)90054-U
11. De Clercq E (2003) Clinical potential of the acyclic nucleoside phosphonates cidofovir, adefovir, and tenofovir in treatment of DNA virus and retrovirus infections. Clin Microbiol Rev 16:569–596. doi:10.1128/CMR.16.4.569-596.2003

12. Kishimoto H, Kojima T, Watanabe Y, Kagawa S, Fujiwara T, Uno F et al (2006) *In vivo* imaging of lymph node metastasis with telomerase-specific replication-selective adenovirus. Nat Med 12:1213–1219. doi:10.1038/nm1404
13. Reid T, Galanis E, Abbruzzese J, Sze D, Wein LM, Andrews J et al (2002) Hepatic arterial infusion of a replication-selective oncolytic adenovirus (dl1520): phase II viral, immunologic, and clinical endpoints. Cancer Res 62:6070–6079
14. Whitley RJ, Roizman B (2001) Herpes simplex virus infection. Lancet 357:1513–1518. doi:10.1016/S0140-6736(00)04638-9
15. Biron KK (2006) Antiviral drugs for cytomegalovirus diseases. Antivir Res 71:154–163. doi:10.1016/j.antiviral.2006.05.002
16. Naesens L, Lenaerts L, Andrei G, Snoeck R, Van Beers D, Holy A et al (2005) Antiadenovirus activities of several classes of nucleoside and nucleotide analogues. Antimicrob Agents Chemother 49:1010–1016. doi:10.1128/AAC.49.3.1010-1016.2005
17. Morfin F, Dupuis-Girod S, Mundweiler S, Falcon D, Carrington D, Sedlacek P et al (2005) *In vitro* susceptibility of adenovirus to antiviral drugs is species-dependent. Antivir Ther 10:225–229
18. Kinchington PR, Araullo-Cruz T, Vergnes JP, Yates K, Gordon YJ (2002) Sequence changes in the human adenovirus type 5 DNA polymerase associated with resistance to the broad spectrum antiviral cidofovir. Antivir Res 56:73–84. doi:10.1016/S0166-3542(02)00098-0
19. Toth K, Spencer JF, Dhar D, Sagartz JE, Buller RM, Painter GR et al (2008) Hexadecyloxypropyl-cidofovir, CMX001, prevents adenovirus-induced mortality in a permissive, immunosuppressed animal model. Proc Natl Acad Sci U S A 105:7293–7297. doi:10.1073/pnas.0800200105
20. Gordon YJ, Araullo-Cruz TP, Johnson YF, Romanowski EG, Kinchington PR (1996) Isolation of human adenovirus type 5 variants resistant to the antiviral cidofovir. Invest Ophthalmol Vis Sci 37:2774-2778

Preclinical evaluation of synergistic effect of telomerase-specific oncolytic virotherapy and gemcitabine for human lung cancer

Dong Liu,[1,3] Toru Kojima,[1,2] Masaaki Ouchi,[4] Shinji Kuroda,[1,2] Yuichi Watanabe,[2,4] Yuuri Hashimoto,[2,4] Hideki Onimatsu,[4] Yasuo Urata,[4] and Toshiyoshi Fujiwara[1,2]

[1]Center for Gene and Cell Therapy, Okayama University Hospital; [2]Division of Surgical Oncology, Department of Surgery, Okayama University Graduate School of Medicine, Dentistry and Pharmaceutical Sciences, Okayama, Japan; [3]Research Center of Lung Cancer, Shanghai Pulmonary Hospital, The Tongji University, Shanghai, China; and [4]Oncolys BioPharma, Inc., Tokyo, Japan

Abstract

A phase I dose-escalation study of telomerase-specific oncolytic adenovirus, OBP-301 (Telomelysin), is now under way in the United States to assess feasibility and to characterize its pharmacokinetics in patients with advanced solid tumors. The present preclinical study investigates whether OBP-301 and a chemotherapeutic agent that is commonly used for lung cancer treatment, gemcitabine, are able to enhance antitumor effects *in vitro* and *in vivo*. The antitumor effects of OBP-301 infection and gemcitabine were evaluated by 2,3-bis[2-methoxy-4-nitro-5-sulfophenyl]-2H-tetrazolium-5-carboxanilide inner salt assay. *In vivo* antitumor effects of intratumoral injection of OBP-301 in combination with systemic administration of gemcitabine were assessed on *nu/nu* mice s.c. xenografted with human lung tumors. OBP-301 infection combined with gemcitabine resulted in very potent synergistic cytotoxicity in human lung cancer cells. The three human lung cancer cell lines treated with OBP-301 for 24 hours tended to accumulate in S phase compared with controls. The proportion of cells in S phase increased from 43.85% to 56.41% in H460 cells, from 46.72% to 67.09% in H322 cells, and from 38.22% to 57.67% in H358 cells. Intratumoral injection of OBP-301 combined with systemic administration of gemcitabine showed therapeutic synergism in human lung tumor xenografts. Our data suggest that the combination of OBP-301 and gemcitabine enhances the antitumor effects against human lung cancer. We also found that the synergistic mechanism may be due to OBP-301–mediated cell cycle accumulation in S phase. These results have important implications for the treatment of human lung cancer. [Mol Cancer Ther 2009;8(4):980–7]

Introduction

Lung cancer is the most common cause of cancer-related mortality. In current clinical practice, chemotherapy is used in combination with radiotherapy as an adjuvant or neoadjuvant therapy. Moreover, combination chemotherapy is regarded as the standard care in the treatment of unresectable locally advanced (stage IIIB), metastatic (stage IV), or recurrent disease. Although there have been major improvements over recent decades in surgical techniques and the role of chemotherapy-radiotherapy in the treatment of non–small cell lung cancer, the long-term outlook for such patients has not changed significantly. The median survival for patients with advanced-stage non–small cell lung cancer treated with platinum-based chemotherapy is a disappointing 8 to 10 months (1). Clearly, new therapies are needed that are capable of treating such advanced cancers in addition to preventing their formation.

One type of cancer therapy that has been extensively investigated is virotherapy, which uses oncolytic viruses engineered to selectively replicate within tumor cells, killing them. We previously developed an adenovirus vector that drives the *E1A* and *E1B* genes under the hTERT promoter, designated OBP-301 (Telomelysin), and showed its selective replication, as well as its profound cytotoxic activity, in a variety of human cancer cells (2–5). Although the development of OBP-301 as a monotherapy is currently under way clinically based on the promising preclinical results, multimodal strategies to enhance antitumor efficacy *in vivo* are essential for successful clinical outcome. In fact, most clinical trials for oncolytic viruses have been conducted in combination with chemotherapy or radiotherapy (6).

Gemcitabine (2,2-difluorodeoxycytidine) is a third-generation agent that has been developed in the past decades. Gemcitabine is a deoxycytidine analogue that has shown efficacy as a treatment for many solid tumors and is now extensively used in the treatment of patients with various tumor types (7, 8), but inherent and acquired resistance has resulted in low response rates. In the present study, we hypothesized that combination of oncolytic adenoviral agents (with novel mechanisms of action) with

Received 9/19/08; revised 12/15/08; accepted 1/20/09.

Grant support: Ministry of Education, Science, and Culture, Japan (T. Fujiwara); Ministry of Health and Welfare, Japan (T. Fujiwara); and Japan China Medical Association (D. Liu).

The costs of publication of this article were defrayed in part by the payment of page charges. This article must therefore be hereby marked *advertisement* in accordance with 18 U.S.C. Section 1734 solely to indicate this fact.

Requests for reprints: Toshiyoshi Fujiwara, Center for Gene and Cell Therapy, Okayama University Hospital, 2-5-1 Shikata-cho, Okayama 700-8558, Japan. Phone: 81-86-235-7997; Fax: 81-86-235-7884. E-mail: toshi_f@md.okayama-u.ac.jp

doi:10.1158/1535-7163.MCT-08-0901

chemotherapeutic agents could improve the antitumor effects and minimize the toxic side effects of the latter by reducing the concentrations of anticancer drugs. To test our hypothesis, we examined the therapeutic effects of OBP-301 combined with gemcitabine both *in vitro* and *in vivo*. The results showed that combination therapy with OBP-301 and gemcitabine produced therapeutic benefits over either individual modality.

Materials and Methods

Cell Lines and Cell Cultures

The human large cell lung cancer cell line H460, the bronchioloalveolar carcinoma cell line H322, and the bronchioloalveolar carcinoma cell line H358 were propagated in monolayer culture in RPMI 1640 supplemented with 10% FCS.

Chemotherapeutic Agents and Viruses

Gemcitabine (Gemzar) was obtained from Eli Lilly Co. Stock solution was prepared in 0.9% NaCl and the agent was further diluted in growth medium immediately before use. OBP-301 is a telomerase-specific replication-competent adenovirus variant, in which the hTERT promoter element drives the expression of *E1A* and *E1B* linked with internal ribosomal entry site. The virus was purified by ultracentrifugation in cesium chloride step gradients and titer was determined by plaque assay in 293 cells, as described previously (2–5).

Cell Viability Assay

2,3-Bis[2-methoxy-4-nitro-5-sulfophenyl]-2H-tetrazolium-5-carboxanilide inner salt (XTT) assay was done to assess the viability of tumor cells. H460, H322, and H358 cells at 1,000 per well were seeded onto 96-well plates at 18 to 20 h before viral infection. Cells were then infected with OBP-301 at low to high concentrations and were treated with fresh medium containing gemcitabine at various concentrations at 24 h after OBP-301 infection. Cell viability was determined at 4 d after treatment with OBP-301 and gemcitabine by using a Cell Proliferation Kit II (Roche Molecular Biochemicals) according to the protocol provided by the manufacturer.

In vitro Replication Assay

H460, H322, and H358 cells were seeded in six-well plates at 10^5 per well at 12 h before infection. Cells were infected with OBP-301 at a multiplicity of infection (MOI) of 10, 25, and 20 plaque-forming units (pfu)/cell, respectively, and fresh medium containing gemcitabine at 70 nmol/L for H460 cells, 100 nmol/L for H322 cells, and 3 nmol/L for H358 cells was then added at 24 h after infection. Cells were incubated at 37°C, trypsinized, and harvested for intracellular replication analysis at 2, 24, 48, 72, 96, and 108 h after OBP-301 infection. DNA purification was done using QIAmp DNA Mini kit (Qiagen, Inc.). The E1A DNA copy number was determined by quantitative real-time PCR using a LightCycler instrument and LightCycler-DNA Master SYBR Green I (Roche Diagnostics).

Assessment of E1A Expression by Western Blotting

H460, H322, and H358 cells infected with OBP-301 at an MOI of 10, 25, and 20, respectively, were collected at 5 d after infection, lysed in lysis buffer [10 mmol/L Tris-HCl (pH 7.5), 400 mmol/L NaCl, 1 mmol/L DTT, 5 mmol/L NaF, 1 mmol/L EDTA, 0.5% Na_3VO_4, 10% glycerol, 0.5% NP40, 0.1 mmol/L phenylmethylsulfonyl fluoride, 1 mg/mL leupeptin, 1 mg/mL aprotinin] for 30 min on ice, and centrifuged at 15,000 rpm for 30 min. Protein concentration was measured by means of the Bradford assay. Equal amounts of protein-containing sample buffer [62.5 mmol/L Tris-HCl (pH 6.8), 2% SDS, 10% glycerol, 5% β-mercaptoethanol] were boiled for 5 min and electrophoresed under reducing conditions on 12% (w/v) polyacrylamide gels. Proteins were electrophoretically transferred to Hybond polyvinylidene difluoride transfer membranes (Amersham) and incubated with primary antibody against E1A (BD Pharmingen) or rabbit anti-human β-actin monoclonal antibody (Sigma-Aldrich) followed by peroxidase-linked secondary antibody. An enhanced chemiluminescence Western system (Amersham) was used to detect secondary probes.

Cell Cycle Analysis

H460, H322, and H358 cells were infected with OBP-301 at 40, 100, and 80 MOI, respectively, for 24 h. The cells were then harvested and suspended in 1.5 mL PBS before fixing with ice-cold 70% ethanol for 30 min. Fixed samples were centrifuged for 5 min, and cell pellets were resuspended in 700 μL PBS containing RNase (0.25 mg/mL) followed by incubation for 30 min at 37°C. The volume was increased to 1 mL with PBS containing 1% bovine serum albumin and propidium iodide (50 μg/mL) and the suspensions were incubated at 4°C for 30 min. Stained cells were analyzed by FACScan (Becton Dickinson) and by WinMDI v2.8 software (Scripps Institute).

Assessment of Cell Cycle Regulator Protein Expression by Western Blotting

H460, H322, and H358 cells were infected with OBP-301 at 40, 100, and 80 MOI, respectively, before harvesting 24 h later. Collected cells were analyzed for expression of E2F1, p53, and E1A and phosphorylation of Akt. Primary antibodies were purchased from Santa Cruz Biotechnology (E2F1), Calbiochem Co. (p53), and Sigma Co. (β-actin). Protein expression was quantified by densitometric scanning using NIH Image software.

In vivo Human Tumor Model

H358 cells (5×10^6 per mouse) were injected s.c. into the backs of 5- to 6-wk-old female BALB/c *nu/nu* mice and were permitted to grow to 5 to 10 mm in diameter. At that time, mice were randomly assigned into four groups: mock, OBP-301, gemcitabine, and OBP-301 plus gemcitabine. Next, 50 μL of solution containing OBP-301 at a dose of 1×10^7 pfu/body or PBS were injected into the tumors. Simultaneously, each mouse in the combination group and gemcitabine group received an i.p. injection of 100 μL gemcitabine at a dose of 70 mg/kg every 3 d for three cycles starting at day 0. The perpendicular

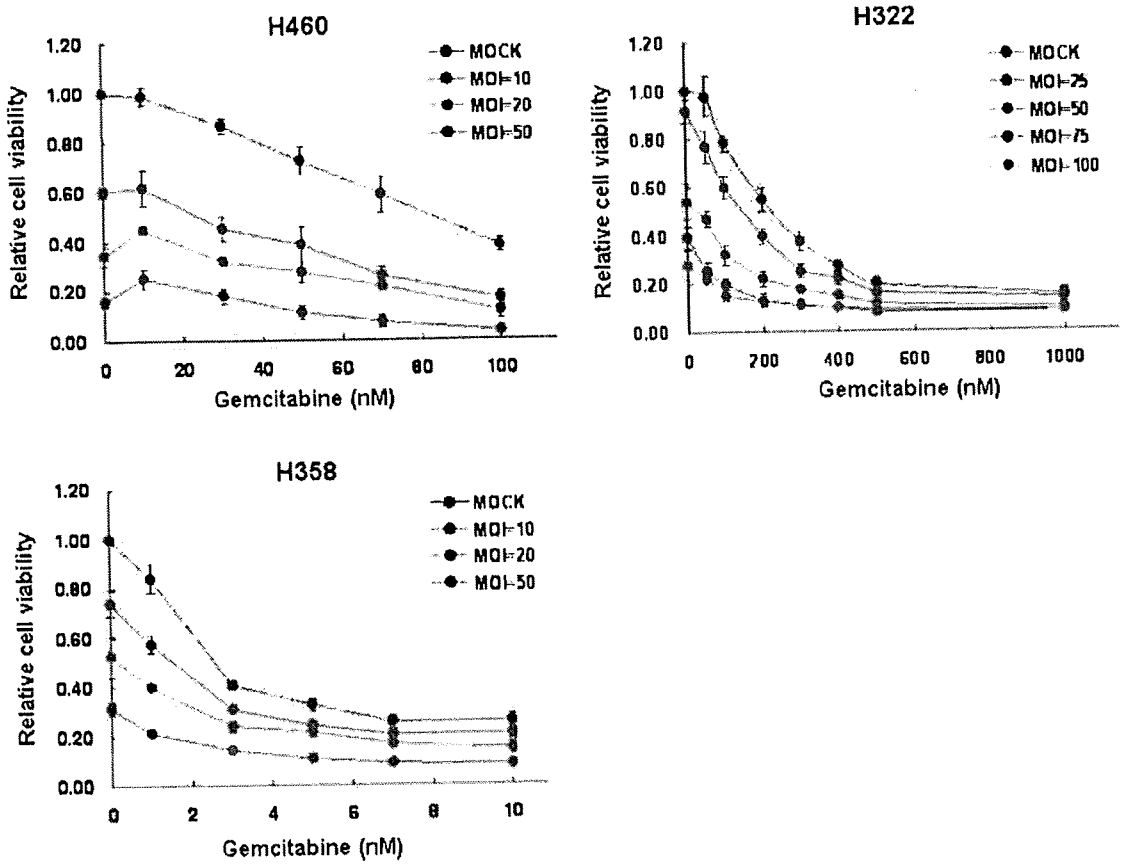

Figure 1. Combination efficiency of OBP-301 and gemcitabine on human lung cancer cell lines. H460, H322, and H358 cells were infected with OBP-301 at the indicated MOIs and then exposed to gemcitabine at the indicated concentrations at 24 h after infection. Cell viability was assessed by XTT assay at 5 d after OBP-301 infection. *Bars*, SD.

diameter of each tumor was measured every 3 d, and tumor volume was calculated using the following formula: tumor volume (mm^3) = $a \times b^2 \times 0.5$, where a is the longest diameter, b is the shortest diameter, and 0.5 is a constant used to calculate the volume of an ellipsoid. The experimental protocol was approved by the Ethics Review Committee for Animal Experimentation of Okayama University.

Statistical Analysis

Determinations of significant differences in mean tumor size among groups were assessed by calculating the value of Student's t using the original data analysis.

Results

Antitumor Efficacy of OBP-301 Combined with Gemcitabine in Human Lung Cancer Cell Lines *In vitro*

Before we tested the combination efficacy, sensitivity to gemcitabine and OBP-301 was evaluated in a variety of human lung cancer cell lines by the XTT method, and we selected three cell lines, H460, H322, and H358, for further experiments. From the XTT experiments with gemcitabine alone or OBP-301 alone (Supplementary Fig. S1),[5] the optimal concentrations of gemcitabine and OBP-301 were determined for each cell line. To examine the potential interaction between gemcitabine and OBP-301 *in vitro*, cell viability with six to eight different doses of OBP-301 and four to five doses of gemcitabine was then assessed by XTT assay at 5 days after treatment. Representative dose-response curves are shown in Fig. 1. All cell lines treated with OBP-301 and gemcitabine showed reduced viability when compared with cells treated with single agents.

We then used software to analyze the combination efficiency in these three cell lines (Table 1). In H358 cells, OBP-301 and gemcitabine were apparently synergistic at most doses, whereas the effect of the combination was mostly additive in H322 cells. In H460 cells, the effect was additive when the concentration of gemcitabine was 50 nmol/L; with the increasing of the concentration, however, a clear synergistic effect was seen. When the concentration was 100 nmol/L, synergism was apparent. These

[5] Supplementary data for this article are available at Molecular Cancer Therapeutics Online (http://mct.aacrjournals.org/).